Verification of design models for geothermal power plants

Árni Jakob Ólafsson

Faculty of Industrial Engineering,
Mechanical Engineering and
Computer Science
University of Iceland
2014

Verification of design models for geothermal power plants

Árni Jakob Ólafsson

30 ECTS thesis submitted in partial fulfillment of a
Magister Scientiarum degree in Mechanical engineering

Advisor(s)
Halldór Pálsson
Marta Rós Karlsdóttir

Faculty Representative
Guðrún Sævarsdóttir

Faculty of Industrial Engineering,
Mechanical Engineering and Computer Science
School of Engineering and Natural Sciences
University of Iceland
Reykjavik, August 2014

Verification of design models for geothermal power plants
Geothermal power plant design models
30 ECTS thesis submitted in partial fulfillment of a *Magister Scientiarum* degree in Mechanical engineering

Faculty of Industrial Engineering, Mechanical Engineering and Computer Science
School of Engineering and Natural Sciences
University of Iceland
Hjarðarhagi 2-6
107, Reykjavik
Iceland

Telephone: 525 4700

Bibliographic information:
Árni Jakob Ólafsson, 2014, *Verification of design models for geothermal power plants*, Master's thesis, Faculty of Industrial Engineering, Mechanical Engineering and Computer Science, University of Iceland.

Printing: Háskólaprent
Reykjavik, Iceland, september 2014

Abstract

In this thesis it is examined how accurately simple thermodynamic models of a single flash working cycle in a geothermal power plant simulate a working cycle of an actual one. The main purpose is to identify what are reasonable values for important parameters in these models. This is done by comparing model results with actual data from Hellisheiði power plant, located in south-west of Iceland. The results show that a suitable value for the turbine base efficiency in a simple model of a single flash cycle is 0.935, or slightly higher than 0.9, a value commonly used. It was verified that non-condensable gases can be excluded in the model calculations for low gas contents and the pressure drop between the steam separator outlet and the turbine inlet can be neglected. The combined overall heat transfer coefficient for the three step condenser at Hellisheiði power plant was observed to be 1300 W/m^2K which is considerably lower than 2000 W/m^2K, a value commonly used for steam condensers. The results provide estimation for important design parameters and indicate that the most common simplifications made in modeling, are justified. The thesis can serve as a guide when constructing simple thermodynamic models to simulate geothermal power plants.

Útdráttur

Í þessari ritgerð er rannsakað hversu vel einföld varmafræði líkön af eins þrepa hvellsuðu vinnuhring herma raunverulegan vinnuhring í jarðvarmavirkjun. Megintilgangurinn er að meta sennileg gildi á mikilvægum breytum í slíkum líkönum. Þetta er gert með því að bera saman niðurstöður líkana við mæligögn frá Hellisheiðarvirkjun. Niðurstöðurnar sýna að sennilegt gildi fyrir grunn nýtni hverfils í einföldu líkani af eins þrepa hvellsuðu vinnuhring er 0.935, eða aðeins hærra en venjulega er notast við. Einnig var sannreynt að ekki er þörf á að gera ráð fyrir óþéttanlegum gösum í útreikningum slíkra líkana ef massa hlutfall þeirra er lítið og að ekki er þörf á að gera ráð fyrir þrýstifalli í pípum og búnaði milli úttaks gufuskilju og inntaks hverfils. Sameiginlegur heildar varmaflutnings stuðull fyrir þriggja þrepa eimsvala í Hellisheiðarvirkjun var reiknaður 1300 W/m^2K sem er töluvert lægra gildi en almennt er notað fyrir vatnsgufu-eimsvala. Niðurstöðurnar gefa mat á mikilvægum hönnunarbreytum og gefa í skyn að flestar einfaldanir sem gerðar eru í slíkum líkönum hafi rétt á sér. Ritgerðin hefur notagildi sem leiðbeiningarskjal við smíði á einföldum varmafræði líkönum til að herma jarðvarmavirkjanir.

Table of Contents

List of Figures

List of Tables

Nomenclature

A	Area of heat exchange [m^2]
C	Capacity rate [kJ/(sK)]
c	specific heat [kJ/(kgK]
C_{min}	Capacity rate of a minimum fluid [kJ/(sK)]
C_{max}	Capacity rate of a maximum fluid [kJ/(sK)]
C_r	Capacity rate ratio
EES	Engineering Equation Solver
g	Subscript for gas
h	enthalpy [kJ/kg]
l	Subscript for liquid
$\dot{m}$	Mass flow [kg/s]
N	Number of Transfer Units
NTU	Number of Transfer Units
o	opening ratio of a control valve [%]
P	Pressure [bar-a]
$\dot{Q}$	Heat transferred [kW]
$\dot{Q}_C$	Condenser heat transfer [kW_{th}, MW_{th}]
s	Entropy [kJ/(kg•K)]
T	Temperature [°C, K]
U	Overall heat transfer coefficient [$W/(m^2•K)$]
v	Specific volume [m^3/kg]
$\dot{v}$	Volumetric flow [l/s]
$\dot{W}$	Work per unit time [kW]
$\dot{W}_e$	Electric power output [kW]
$\dot{W}_s$	Isentropic power output [kW]

x	Steam quality

Greek Symbols

ϵ	Heat exchanger effectiveness
η	Efficiency
η_0	Base efficiency
η_g	Generator efficiency
η_m	Mechanical efficiency
$\eta_{m,g}$	Combined mechanical and generator efficiency
η_s	Isentropic efficiency

Nomenclature in Figures

HPS	High Pressure Separator
HPM	High Pressure Moisture remover
HPT	High Pressure Turbine
C	Condenser
CP	Condenser Pump
CWP	Cold Water Pump
WV	Wellhead Valve

Acknowledgements

I would like to thank my supervisors Associate Professor Dr. Halldór Pálson at the Department of Mechanical and Industrial Engineering at the University of Iceland and Marta Rós Karlsdóttir, Phd student at the Department of Mechanical and Industrial Engineering at the University of Iceland and Director of Resources at the Icelandic energy company Our Nature, for their guidance and assistance.

Furthermore I would like to thank Kristinn Rafnsson production manager at Our Nature for provision of data logged at Hellisheiði power plant.

Special thanks go to my colleagues at Efla Engineering for their hospitality, provision of facilities and assistance. Namely Rúnar Magnússon director of Geothermal energy and District heating, Heimir Hjartarson, Smári Guðfinnsson, Almar Gunnarsson, Unnar Víðisson and Jón Andri Hjaltason.

I thank Dr. Freyr Harðarson and Gunnlaugur Ó. Ágústsson at Mannvit Engineering for their assistance and provision of data from Hellisheiði power plant. Óskar Pétur Einarsson and Davíð Örn Benediktsson at Verkís Engineering provided some useful insight and assistances and for that they have my gratitude. My friend Magnús Kári Ingvarsson has my gratitude for providing help with Figure 6.4.

My brother in law Dr. Sigurður Örn Stefánsson Assistant Professor at the Department of Physical Sciences at the University of Iceland, has my gratitude for his careful reading of the manuscript.

I am most thankful for the discussions, unconditional support and encouragement from my father, Dr. Ólafur G. Flóvenz, director of Iceland GeoSurvey (ISOR).

1 Introduction

In recent years, renewable energy sources such as geothermal energy have been growing with increased awareness of the harmful effects of fossil fuels on the Earth, its climate and the health of its inhabitants.

Geothermal energy or simply geothermal, is often referred to in modern times as "that part of the Earth's heat that can, or could, be recovered and exploited by man" (Dickson and Fanelli 2004). The term applies to all energy generated and stored within the earth's crust and mantle, mostly by radioactive decay of materials but also includes some heat from the earth's formation, 4.5 billion years ago. Its effects can be seen in many places on the earth's surface as geysers, hot springs and volcanoes, especially near tectonic plate boundaries (Dickson and Fanelli 2004).

The heat in the earth's crust has been estimated to be 5.4 billion EJ and if 0.1% of this energy could be harnessed, it would satisfy the present world's energy consumption for the next 10,000 years. However, harnessing the earth's energy on this scale is extremely difficult and requires improved technology (Flóvenz 2012).

For electricity generation from geothermal to be feasible, a minimum temperature of 150°C is generally needed, although power generation from significantly lower temperatures has been achieved. The temperature gradient of the Earth is 25-30°C/km on average, limiting electricity generation from geothermal to locations with higher temperature gradient to avoid deep drilling (Trinnaman and Clarke 2010).

Due to its geographical location, Iceland has vast geothermal resources. Power generation from geothermal in Iceland has increased steadily, with a current number of five power plants and at least two new plants are to be constructed in the coming years (Pálmason 2005, Landsvirkjun 2013).

When considering geothermal power plants, it is useful to be able to quickly generate a simple thermodynamic model that simulates their working cycle. Models used to accurately model geothermal power plants are complicated and usually only show one component at a time. A simple model of the working cycle can give an estimation of what to expect from the power plant based on the properties of the geothermal fluid. The question that remains however is, how accurate and reliable are those models?

The goal of the study is to see how simple thermodynamic models of a single flash power plant estimate the working cycle of an actual geothermal single flash cycle, what assumptions need to be made and if common simplifications have any significant effects. The main objectives are

- To find a reasonable value for the base efficiency of a turbine η_0, to use when making simple models of geothermal power plants.
- To examine the effects of excluding pressure drop between the steam separator and the turbine in simple models.

- To examine the effects of excluding the non-condensable gases in the steam in simple models.
- To use measured values for the energy transfer in the condenser to verify the steam quality and enthalpy at the condenser inlet, that is calculated using the Baumann rule.
- To compare the overall coefficient of heat transfer in each step of the condenser to values commonly used for condensers in geothermal power plants.

The thesis is organized as follows.

Chapter 2 is reserved for discussion on geothermal energy on a global scale, classifications of geothermal energy systems and the history of- and current geothermal utilization both in Iceland and worldwide. Chapter 3 describes both single- and double flash geothermal power plants, their components and the thermodynamics of their working cycles. The last subsection describes Hellisheiði power plant. Chapter 4 describes the methods used to achieve the objectives listed in the introduction. Chapter 5 presents the data gathered, its stability, which measurements are used and how they are handled. Chapter 6 presents the results of the research conducted and simulations, comparison of various parameters and discussion. Chapter 7 shows the conclusions drawn from the results and suggestions for further research.

2 Geothermal Energy

Geothermal systems can be grouped into a few categories. The main source of geothermal energy production comes from hydrothermal systems that are driven by natural flow of hot water. Other systems include enhanced geothermal systems (EGS) and hot dry rock (HDR) (DiPippo 2007). In enhanced geothermal systems, natural permeability is too low for efficient production and requires enhancement by engineering the reservoir. Hot dry rock contains almost no natural permeability but sufficient temperature for energy production (Flóvenz 2014).

It is customary to classify geothermal systems according to reservoir temperature. Traditionally, high temperature fields are defined as fields where the temperature exceeds 200°C at 1 km depth. The classification of systems with lower temperature is not well defined and varies between authors. A geothermal system with temperature in the range 100-200°C at 1 km depth is commonly referred to as an intermediate system or a boiling low temperature field. If the temperature at 1 km depth is below 100°C the system is usually classified as a low temperature system (Pálmason 2005).

High temperature fields are mainly located on plate boundaries or associated with active or recent volcanism. The crust in high temperature fields is fractured and permeable to water and gives rise to convective heat transfer, where energy is extracted from a heat source at depth towards shallower depths and surface. The heat sources of high temperature fields are usually cooling intrusions or magma chambers (Flóvenz 2014).

The low and intermediate temperature fields can either be convective fracture dominated systems in basement rock or embedded in thick and permeable sedimentary basins. In both cases, the heat is derived from the general crustal heat flow (Flóvenz 2014).

2.1 Geothermal utilization worldwide

Geothermal energy has been utilized by man for thousands of years. In ancient times hot springs were used for bathing, washing, volcanic rock used for making weapons and hot rocks used for cooking (Arriaga 2005).

Geothermal energy was first used for district heating on a large scale in Idaho, USA in 1892 followed by heating of greenhouses and other buildings in Tuscany, Italy (Dickson and Fanelli 2004), and exploitation of geothermal for domestic heating in Iceland in 1928 (Pálmason 2005).

The birth of electricity generation from geothermal energy can be traced back to the Larderello region in Italy where in 1904 the first experiment to produce electricity from geothermal energy was conducted. The following year the first geothermal power plant prototype went into operation in the region and in 1913 the first commercial plant became operational (Dickson and Fanelli 2004, Lund 2006).

The success of these experiments led to small scale electricity production from geothermal in Beppu, Japan in 1919 and at the geysers in California in 1921. Wairakei station in New Zealand became operational in 1958 and was the first plant to utilize wet steam (flash steam technology) for electricity production, a turning point in the history of the technology. The previous plants were all restricted to the use of geothermal reservoirs that contained dry steam (Dickson and Fanelli 2004). Installed capacity worldwide over the period 1950 to 2015 is shown in Figure 2.1, where the percentage number represents the increase in installed capacity over the preceding five year period with the red bar representing the forecast for the end of year 2015.

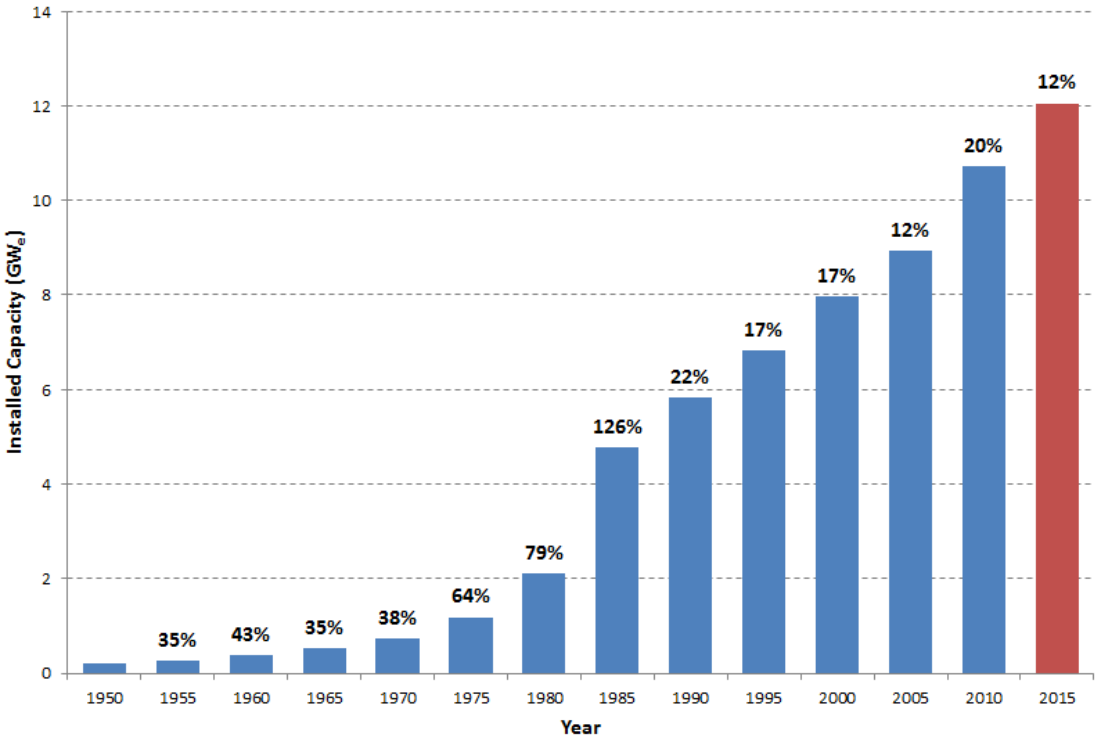

Figure 2.1 *Worldwide installed geothermal electric capacity and percentage increase every five years (Bertani 2014)*

In the decades following the commission of the Wairakei power plant, geothermal utilization increased steadily until the 1980s where the increase became rapid as shown in Figure 2.1 partially in response to the oil crises during the 80's. In 1977, the first double flash power plant became operational in Japan and in 1984, geothermal power plants using binary cycles were introduced (Bertani 2010). The binary cycle allows the use of cooler geothermal water than necessary for conventional steam turbines and improves efficiency of existing power plants if used as bottoming cycles.

Electricity from geothermal energy has been produced in 27 countries worldwide and the total installed capacity was 10,715 MW in 2010, with a distribution of 41% single flash, 27% dry steam, 20% double flash, 11% binary/combined cycle/hybrid and 1% backpressure (Bertani and Lund 2010). Current forecasts suggest an increase in installed capacity worldwide reaching 12 GW by the end of 2015 (Bertani 2014).

Most of the installed capacity is distributed among relatively few nations, Table 2.1 shows the power generation of the leading nations in 2010 and their expected power generation by the end of 2015.

Table 2.1 *Installed electric capacity of leading nations (Bertani 2014)*

Country	**Installed capacity in 2010 (MW)**	**Forecast of installed capacity in 2015 (MW)**
USA	3093	3408
Philippines	1904	1904
Indonesia	1197	1222
Mexico	958	1014
Italy	843	876
New Zealand	628	782
Iceland	575	665
Japan	536	537
El Salvador	204	204
Kenya	167	532
Turkey	82	247
Others	528	662
Total	10715	12053

2.2 Geothermal utilization in Iceland

Iceland is located on the Mid-Atlantic Ridge, on the North American and Eurasian tectonic plate boundary and thus has very favorable conditions for geothermal utilization. The country is relatively young geologically and is one of the most tectonically active countries in the world, with over 200 volcanoes located on the active zone, frequent earthquakes, numerous hot springs and at least 20 high temperature areas with temperatures reaching 250°C at less than 1 km depth (Ragnarsson 2010). High temperature fields in Iceland are usually under pressurized and water dominated, frequently following a boiling point depth curve (Pálmason 2005).

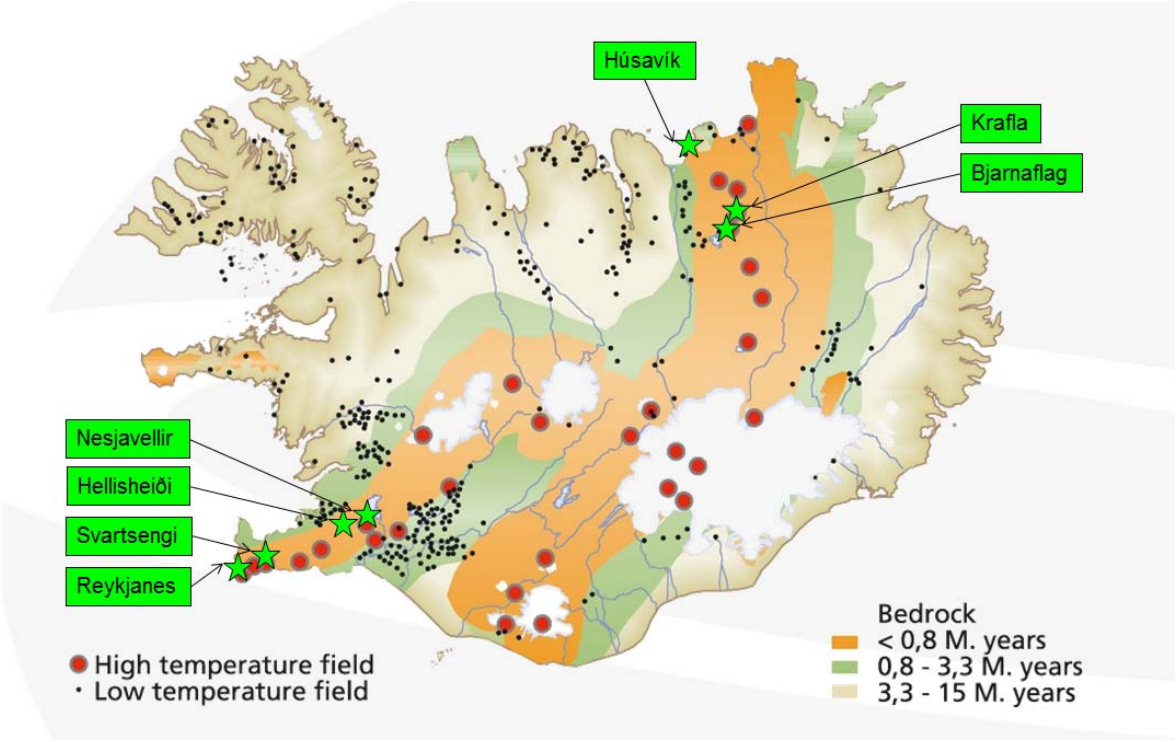

Figure 2.2 *Geological map of Iceland (courtesy of ISOR - Iceland GeoSurvey)*

As of 2010, the total installed electrical capacity from geothermal resources was 573 MW and 62% of the countries primary energy comes from geothermal, with district heating playing a large part as 89% of houses are heated in this manner (Ragnarsson 2010). The installed electric capacity has since increased to 664 MW. The distribution of electricity generation and power plant types can be seen in Table 2.2.

Table 2.2 *Electricity generation from geothermal power plants in Iceland (Flóvenz 2012, Pálsson 2012)*

Power plant	**Installed capacity (MW)**	**Type**
Hellisheiði	303	Single and double flash
Nesjavellir	120	Single flash
Reykjanes	100	Single flash
Svartsengi	76	Single flash and binary
Krafla	60	Double flash
Bjarnarflag	3	Single flash
Húsavík	2	Kalina
Total	664	

There are currently two power plants under development, at Þeistareykir and Bjarnarflag. The first step in that project will be the installation of a 45 MW power plant at either location with possible further installments. Þeistareykir area is believed to be able to sustain up to 270 MW of electricity production (Landsvirkjun 2013). The capacity at Bjarnarflag will be increased to 45-90 MW with the installation of at least one 45 MW turbine in the coming years (Mannvit 2011).

3 Geothermal power plants

In this chapter, the thermodynamics that govern the processes in geothermal power plants is explained. The main characteristics and components of both single and double flash power plants are listed and explained.

3.1 Theoretical background

Geothermal power plant operation cycles follow the basic laws of thermodynamics, mainly the conservation of energy. The conservation of mass is also important when analyzing these cycles.

The most important parameters when considering these working cycles are the following fluid properties:

- Pressure, P, is a design parameter with the unit Pa or bar. Bar and bar-a are often used in the geothermal industry. Throughout this thesis, the absolute pressure in bar-a will be used to avoid confusion.

- Temperature, T, is often a constraint in the form of minimum temperature, maximum temperature or temperature difference. The unit is °C or K. Throughout this thesis, the unit °C is used.

- Enthalpy, h, describes the energy content of a unit mass of flowing fluid. The unit is kJ/kg.

- Entropy, s, describes the disorder of a unit mass of fluid. The unit is kJ/(kgK).

- Specific volume, v, is the ratio of a fluids volume to its mass. The unit is m^3/kg. Specific volume is used to determine flow speed of a fluid through pipelines from mass flow and diameter.

In the operation cycle, the working fluid undergoes phase changes. Generally, there will exist a liquid phase, a gas phase and often a two phase mixture of liquid and gas at some point in the cycle. The steam quality of the gas phase in the two phase mixture is defined as

$$x = \frac{\dot{m}_g}{\dot{m}_g + \dot{m}_l} \qquad 3.1$$

where $\dot{m}$ denotes mass flow and the subscripts l and g denote the properties of liquid and gas respectively. Similarly, steam wetness or water quality is the mass fraction of water in the steam and equals $1 - x$.

The enthalpy, entropy and specific volume of the mixture are described by

$$h = (1 - x)h_l + xh_g \quad 3.2$$

$$s = (1 - x)s_l + xs_g \quad 3.3$$

$$\nu = (1 - x)\nu_l + x\nu_g. \quad 3.4$$

When working with a single phase pure fluid, two fluid properties must be known to calculate the rest. In the case of a two phase pure fluid, two fluid properties must also be known, but the steam quality can be one of them (Pálsson 2012).

In a geothermal power plant working cycle, different thermodynamic processes occur in various components of the plant. These processes are assumed to be ideal i.e. neglecting losses. This provides a good estimation of what occurs in a given component. The most notable processes used when analyzing geothermal power plant working cycles are:

- Isenthalpic processes, where the enthalpy, h, is considered a constant over a given component.
- Isobaric processes, where the pressure, P, is considered a constant over a given component
- Isentropic processes, where the entropy, s, is considered a constant over a given component
- Heat transfer, where heat is transferred to or from the fluid over a given component but no work is transferred.

The mass flow into a component must be equal to the mass flow out of the component, that is

$$\dot{m}_{in} = \dot{m}_{out}. \quad 3.5$$

A fluid with enthalpy h, and mass flow $\dot{m}$, has an energy content equal to $\dot{m}h$ and the first law of thermodynamics states that energy that enters a component must be equal to the energy exiting the component. Therefore

$$\dot{m}_{in}h_{in} = \dot{m}_{out}h_{out} + \dot{W} + \dot{Q} \quad 3.6$$

where $\dot{W}$ denotes the work done per unit time by the fluid passing through the component ($\dot{W} > 0$) or work applied to the fluid ($\dot{W} < 0$) and $\dot{Q}$ denotes the heat transferred from the fluid ($\dot{Q} > 0$) to the surroundings or to the fluid from the surroundings ($\dot{Q} < 0$). Equations 3.5 and 3.6 hold for all components in steady processes and can consequently be used to determine unknown properties in the analysis of the process in question (Pálsson 2012).

Thermal efficiency η_{th}, of a process, is a measure of the process quality and is defined as the ratio between the work output and the heat flow into the process. That is

$$\eta_{th} = \frac{\dot{W}}{\dot{Q}_{in}} = \frac{\dot{Q}_{in} - \dot{Q}_{out}}{\dot{Q}_{in}}. \quad 3.7$$

Isentropic efficiency η_s, measures a process quality compared to the theoretical maximum performance of an ideal, reversible process where no losses occur, or

$$\eta_s = \frac{\dot{W}}{\dot{W}_s} = \frac{\dot{m}_{in}(h_{in} - h_{out})}{\dot{m}_{in}(h_{in} - h_{s,out})}. \quad 3.8$$

$\dot{W}$ denotes the actual power output of the turbine and $\dot{W}_s$ and $h_{s,out}$ denote the turbines power output and outlet enthalpy respectively, assuming the process ideal.

3.2 Single-flash power plants

Single-flash power plants utilize steam between two pressure levels to generate electricity by rotating a turbine and are the most common power plant types, accounting to 32% of all power plants and 42% of all installed geothermal power worldwide. A single-flash power unit is typically around 25 MW_e but can range from 3 to 90 MW_e (DiPippo 2007).

The term single-flash refers to that the pressurized liquid has been flashed once into a steam and liquid mixture by reducing the pressure of the liquid below the saturation pressure of water for a given temperature. Flashing can occur in the reservoir, in the production well, in the gathering pipes leading to a steam separator or at the separator inlet. With extended exploitation of the reservoir over the power plants lifetime, reservoir pressure drops, causing the flashing to "move back" and occur in the production well or the reservoir itself. To maintain reservoir pressure, re-injection of fluid into the reservoir is common (DiPippo 2007).

Condensing power plants

By far the most common geothermal power plant cycle is the condensing power plant which is the focus of this thesis. The steam exiting the turbine enters a condenser that is under-pressurized, usually at around 0.1 bar-a, increasing the pressure drop across the turbine. These plants are more expensive than e.g. backpressure plants since they include the condenser, cooling tower and other cold end components. Typically, around 4.6% of a condensing power plants electricity generation is needed to power the additional components (Dickson and Fanelli 2003). A simple schematic of the working cycle of a single flash condensing power plant is shown in Figure 3.1 below.

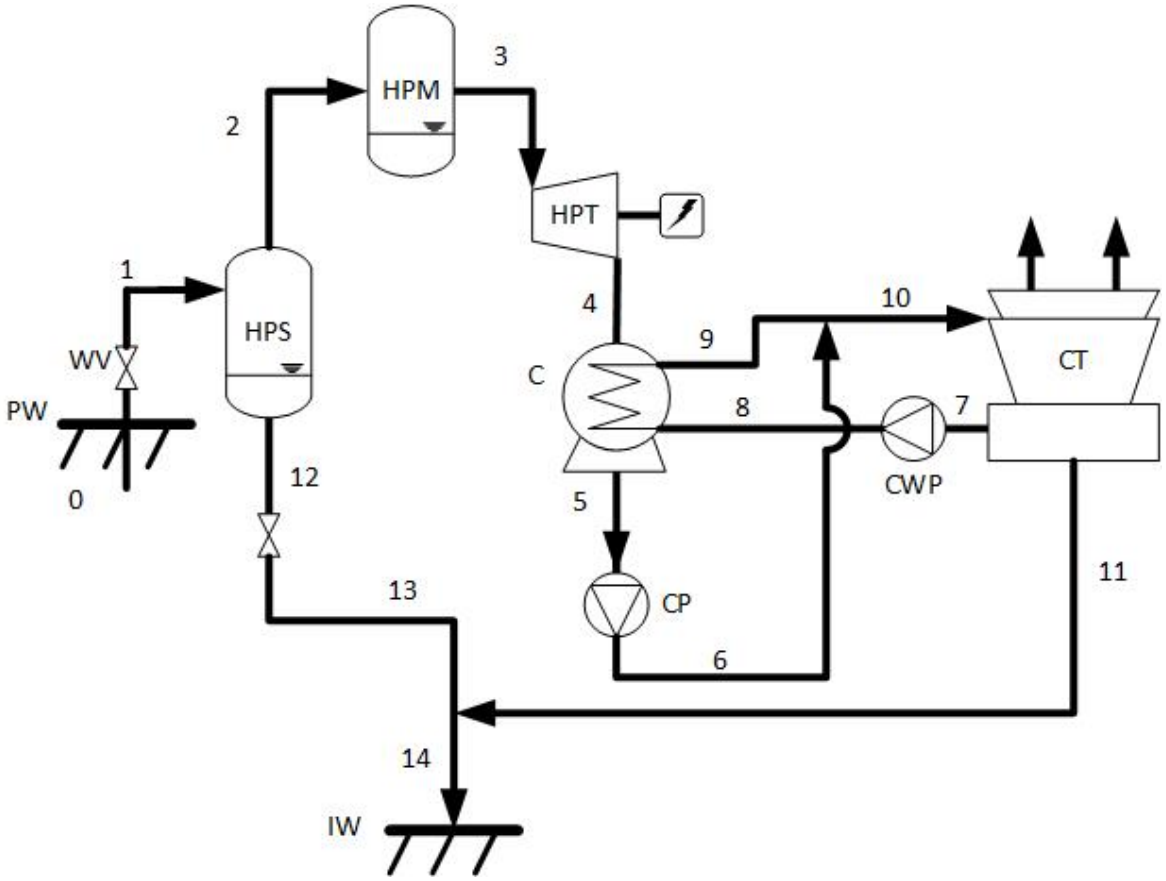

Figure 3.1 *A simple schematic of a single flash condensing power plant*

The process shown in Figure 3.1 is described in the following sections.

3.2.1 Steam gathering systems

The steam-liquid mixture extracted from the production well (PW) in Figure 3.1, is lead to a high pressure steam separator (HPS), where the phases separate due to their density difference. There are three main separator layout systems for single flash power plants. A system with one common separator for all production wells located close to the powerhouse, a system with separators at each production well and a satellite system with common separators in the field. In a satellite system, flow from several wells is gathered into a common separator in the field. The steam flows from the separator outlet towards the power station and the separated liquid towards the reinjection wells (DiPippo 2007). This system is used at the Icelandic power plant Hellisheiði (Jóhannesson and Guðmundsson 2012), which is the focus of this thesis.

3.2.2 The working cycle of a single flash condensing power plant

As shown in Figure 3.1, the steam is lead from the steam separator to a high pressure moisture remover (HPM), where droplets and moisture are removed from the steam. The steam then flows into the high pressure steam turbine (HPT), where it expands and rotates the rotor blades to generate electricity.

Some pressure drop will occur in the pipelines and components between the separator and turbine and these pressure drops can cause significant harm to the turbine. Lowering the pressure can cause the steam to become superheated. As the steam dries, dissolved minerals such as silica become dust and damage the turbine. To prevent this, the pipe insulation must be moderate, so that condensation due to the heat loss through the pipe walls matches the boiling caused by the pressure drop (Jóhannesson and Guðmundsson 2012).

At the turbine outlet, the steam is condensed in a condenser (C). Most of the modern condensers are closed shell and tube heat exchangers where the cooling water and geothermal water never come in contact with each other. This enables easier non-condensable gas removal (DiPippo 2007).

The condensing steam is sometimes used to pre heat cold groundwater for district heating. The pre heated groundwater is then lead towards the high pressure separator liquid outlet and heated to sufficient temperature. The condensed steam is lead through a pump (CP), to the cooling tower (CT), where a portion of it recirculates after cooling sufficiently, reducing the volume of cooling water needed (DiPippo 2007).

3.2.3 Plant components and thermodynamics

The state of the geothermal fluid at different points in the power plant's working cycle and the processes it undergoes is described on a thermodynamic state diagram, Figure 3.2.

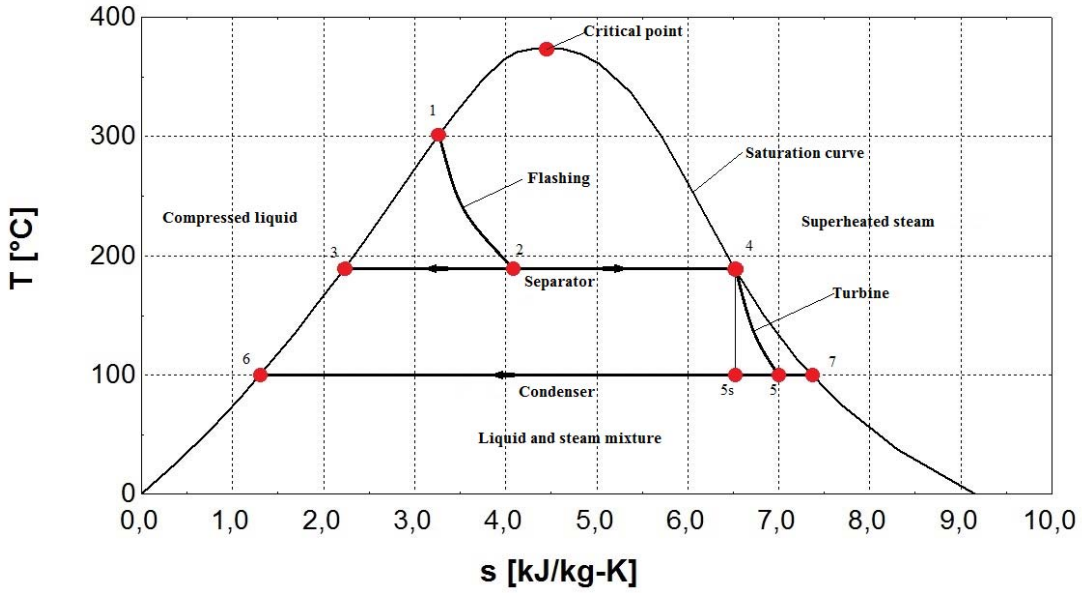

Figure 3.2 *s-T diagram for a single flash condensing power plant*

The mixture is flashed on its way from the geothermal well (point 1) to the separator (point 2) under constant enthalpy. The separated liquid exits the separator (point 3) and the steam flows towards the turbine (point 4). In an ideal turbine, the steam expansion is isentropic, following the curve between points 4 and 5s. In practice however, a more accurate expansion is the one shown by the curve between points 4 and 5. The expanded steam is

then condensed into liquid under constant pressure in the condenser between points 5 and 6.

Production and injection wells

The geothermal well is basically a vertical pipe transporting fluid between the reservoir and the surface. The state of the fluid at the wellhead is important, namely pressure, mass flow and enthalpy. The maximum pressure at the wellhead is limited by the pressure in the reservoir but the pressure can be reduced with a wellhead valve. Temperature in the reservoir is often assumed to be the saturation temperature of water at reservoir pressure to give an estimate of the specific enthalpy in the well. Due to relatively small heat loss through the walls of the well, the enthalpy of the fluid is considered to be constant up the well (Pálsson 2012).

Steam separators

The steam separators utilize the density difference between liquid and gas to separate the two-phase flow into separate liquid and gas phases as shown in Figure 3.3.

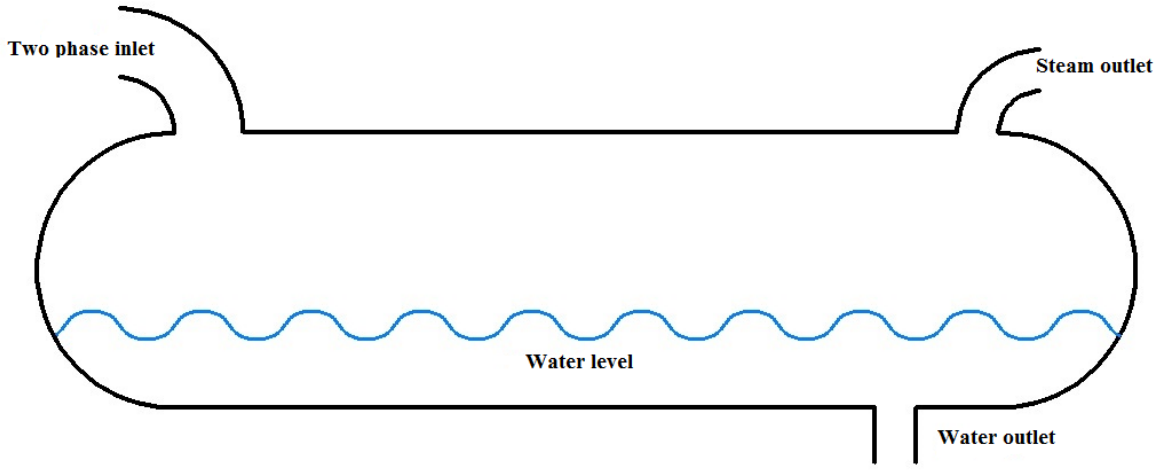

Figure 3.3 *Horizontal drum separator*

The fluid and steam at the outlets in an ideal separator are considered to be saturated and the separation process is assumed to be isobaric. This is however not the case and a rule of thumb states that on average the pressure drop across a separator is roughly 1 bar (Jóhannesson 2012). Several types of separators are common, the most prominent are the horizontal drum separators and the vertical cyclone separators. Most of the new Icelandic power plants utilize horizontal drum separators, due to their cost efficiency and good performance (DiPippo 2007, Pálsson 2012).

Moisture removers

Moisture removers are similar to separators, situated close to the turbine, designed to remove droplets and moisture from the entering steam.

Turbines

When steam enters a turbine, it expands, reducing its density and pressure significantly. Upon expanding, the steam rotates the rotor blades and gets wetter and thus will contain moisture at the outlet. Turbines are the main components of a geothermal power plant. These components are complex in design and modeling. In this thesis, as well as in the power plant models, a simplified version of a turbine will be used. These simplifications can be applied without sacrificing much accuracy. Changes in potential and kinetic energy of the fluid across the turbine are neglected. Typically, these turbines have an isentropic efficiency of 81-85% and a turbine-generator mechanical efficiency of 96.3% (Dickson and Fanelli 2003).

In an ideal turbine, where the process is reversible and isentropic, the turbine will generate maximum work. No turbine is ideal, and the losses need to be considered, commonly done with the turbine isentropic efficiency parameter η_s, which denotes the ratio between actual work produced and the maximum theoretical work.

If the inlet entropy s_{in}, inlet pressure P_{in} and outlet pressure P_{out} are known and the fluid is considered to be saturated then the ideal outlet entropy is

$$s_{s,out} = s_{in} \tag{3.9}$$

and the ideal outlet enthalpy $h_{s,out}$ can be calculated. From the inlet enthalpy, ideal outlet enthalpy and efficiency, the outlet enthalpy is given by

$$h_{out} = h_{in} - \eta\left(h_{in} - h_{s,out}\right). \tag{3.10}$$

The Baumann rule states that for every one percent increase in average steam wetness $1 - x$, in the turbine, there is one percent decrease in turbine efficiency (DiPippo 2007), assuming the steam at the turbine inlet is saturated ($x_{in} = 1$). The efficiency then becomes

$$\eta = \eta_0 - \frac{(1 - x_{in}) + (1 - x_{out})}{2} = \eta_0 - \frac{1 - x_{out}}{2} \tag{3.11}$$

where η_0 is defined as the base efficiency of the turbine.

The Baumann rule can be applied in turbine calculations by using the saturation values of entropy and enthalpy at the outlet pressure to estimate the turbine outlet steam quality. The ideal turbine outlet steam quality is

$$x_{s,out} = \frac{s_{g,in} - s_{l,out}}{s_{g,out} - s_{l,out}} \tag{3.12}$$

where the subscripts g and l denote the gas and liquid phases respectively. The ideal outlet steam quality can be used to determine the ideal outlet enthalpy through Equation 3.2, resulting in

$$h_{s,out} = h_{l,out} + x_{s,out}\left(h_{g,out} - h_{l,out}\right). \tag{3.13}$$

Combining Equations 3.10 and 3.11 results in

$$h_{in} - h_{out} = \left(\eta_0 - \frac{1 - x_{out}}{2}\right)\left(h_{in} - h_{s,out}\right). \quad 3.14$$

The real turbine outlet enthalpy from Equation 3.2 becomes

$$h_{out} = h_{l,out} + x_{out}\left(h_{g,out} - h_{l,out}\right). \quad 3.15$$

Combining Equations 3.14 and 3.15, yields the turbine outlet steam quality

$$x_{out} = \frac{h_{in} - h_{l,out} - \left(\eta_0 - \frac{1}{2}\right)\left(h_{in} - h_{s,out}\right)}{h_{g,out} - h_{l,out} + \frac{h_{in} - h_{s,out}}{2}}. \quad 3.16$$

The outlet steam quality can then be substituted into equation 3.15 to calculate the outlet enthalpy (Pálsson 2012).

Condensers

After exiting the turbine, the steam enters a condenser where it is condensed into liquid under constant pressure, since it greatly reduces work required to pump the fluid. Condensers can either be open where the condensate mixes with cooling fluid (generally water) or closed where the cooling fluid is lead through the condenser in pipes and thus, no mixing occurs. Open condensers are cheap and have good heat transfer characteristics but need regular cleaning and the condensate can only be recovered as overflow from the cooling tower since it mixes with the cooling fluid. Closed condensers are expensive and have poor heat transfer characteristics compared to the open condensers. The condensate does not mix with the cooling fluid and can thus be used for reinjection. Closed condensers require little maintenance and cleaning and are often used to preheat ground water for district heating (Jóhannesson and Guðmundsson 2012). In recent years most new power plants, including Hellisheiði, have used closed condensers partially due to increased reinjection.

Heat exchange calculations of a closed condenser are based on the area of heat transfer, A, and the coefficient of heat transfer for a given heat exchanger. The energy balance of the condenser is

$$\dot{m}_{h,in}\left(h_{h,in} - h_{h,out}\right) = \dot{m}_{c,in}\left(h_{c,out} - h_{c,in}\right) + \dot{Q} \quad 3.17$$

where the subscripts c and h denote cold and hot respectively, hot referring to the condensing fluid and cold referring to the cooling fluid. $\dot{Q}$ denotes heat lost to the environment and is relatively small and is neglected in this study. The condensation takes place at constant temperature. In practice however, the fluid generally cools by a few degrees in the condenser after the condensation takes place (Benediktsson and Einarsson 2014).

Heat exchanger effectiveness ϵ, is defined as the ratio between actual heat transfer and maximum possible heat transfer

$$\epsilon = \frac{T_{c,out} - T_{c,in}}{T_{h,in} - T_{c,in}}. \quad 3.18$$

The maximum possible heat transfer for the exchanger can be achieved if one fluid undergoes a temperature change equal to the maximum temperature difference present in the exchanger which is the difference in the inlet temperature for the hot and cold fluids. The fluid that can achieve this over the exchanger is the one with the lowest capacity rate

$$C = \dot{m}c \quad 3.19$$

where c denotes the specific heat of the fluid. The fluid that undergoes the larger temperature difference in the exchanger is called the minimum fluid and the fluid that undergoes the smaller temperature change is called the maximum fluid. The capacity rates of the minimum and maximum fluids are denoted as $C_{min}$and C_{max} respectively. In the case of a condenser, the cooling fluid is always the minimum fluid. The ratio between the capacity rates of the minimum and maximum fluids is defined as

$$C_r = \frac{C_{min}}{C_{max}}. \quad 3.20$$

As mentioned earlier, the condensation process is assumed to take place at constant temperature, i.e. the condensing fluid behaves as if it has infinite specific heat. Thus, the cooling fluid experiences the most temperature difference and is therefore the minimum fluid. The condensing fluid is then the maximum fluid and as a result, C_r is approximately zero (Holman 2010).

The number of transfer units method is used to analyze the condensers. Number of transfer units, NTU or N, is defined as

$$NTU = \frac{UA}{C_{min}} \quad 3.21$$

where U denotes the heat transfer coefficient of a given heat exchanger and A is the area of heat exchange.

Since the cold fluid is the minimum fluid, combining Equations 3.19 and 3.21 results in

$$NTU = \frac{UA}{\dot{m}_{c,in}c_c}. \quad 3.22$$

Equation 3.23 below holds for all heat exchangers where C_r is zero (Holman 2010).

$$NTU = -\ln(1 - \epsilon). \quad 3.23$$

Substituting equation 3.22 into Equation 3.23 we get

$$\dot{m}_{c,in}c_c = \frac{UA}{\ln(1 - \epsilon)}. \quad 3.24$$

The mass flow of cooling water can be calculated from Equation 3.17 and then the coefficient of heat transfer can be calculated from equation 3.24 (Holman 2010, Pálsson 2012).

Non-condensable gas removal

Non-condensable gases (NCG) are present in the geothermal steam. Since they are non-condensable, they accumulate in the condenser. These gases consist mainly of carbon dioxide (CO_2) and hydrogen sulfide (H_2S) and are removed from the condenser by suction equipment. The non-condensable gas removal is performed in multiple stages, usually two, where the pressure increases to atmospheric. Each stage has an extraction mechanism and a condensation unit (Jóhannesson and Guðmundsson 2012).

Steam ejectors are generally used if the gas content is low (less than 1.5%). They are cheap and reliable extraction mechanisms but are relatively inefficient. Steam ejectors are usually operated in a series of two or three units (Dickson and Fanelli 2003).

Liquid ring vacuum pumps are useful to deal with higher concentration of gas. These devices are expensive and are often used as a second stage, where the first stage extraction is performed by a steam ejector (Dickson and Fanelli 2003).

Compressors are expensive equipment directly coupled to the turbine and are rarely used unless the gas content is extreme, above 20% (Jóhannesson and Guðmundsson 2012).

Cooling towers

Calculations for cooling towers are not included in the models presented in this thesis. Cooling systems are an important part of geothermal power plants however. In the cooling tower, the cooling liquid and sometimes the condensate exiting the condenser is cooled down to be re-injected into the condenser as the cooling fluid. The most common cooling method is to use upward airflow through the tower, causing the condensate to cool and fall to the bottom. These towers have various flow types on which they are categorized (Jóhannesson and Guðmundsson 2012).

3.3 Double-flash power plants

Double flash power plants increase the efficiency of electricity production from the geothermal fluid by flashing the separated liquid a second time under lower pressure. These power plants can produce 15-25% more power than a single flash power plant under the same conditions (DiPippo 2007).

The liquid exiting the steam separator undergoes pressure drop through a throttle valve. As the pressure drops, the liquid boils and a mixture of liquid and steam is formed which then enters a low pressure steam separator. The steam exiting the low pressure separator is then used to produce electricity in a low pressure turbine. The two main types of double-flash power plants are; single unit double-flash plant, where the low pressure steam is lead to the same turbine as the high pressure steam. The alternative, shown on Figure 3.4, is a double unit double-flash plant, where the high and low pressure steams rotate separate turbines.

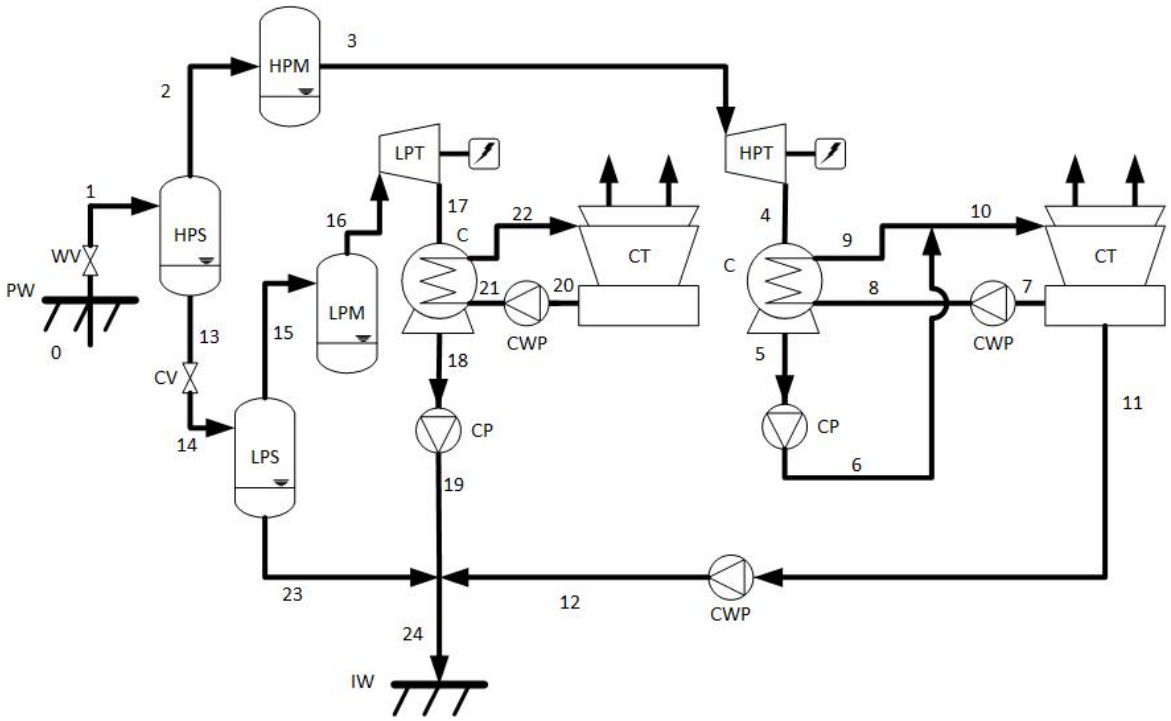

Figure 3.4 *A simple schematic of a double unit double-flash power plant*

Hellisheiði power plant is an example of a double-flash power plant. These plants are similar to single-flash plants and their differences will be described in this chapter.

3.3.1 Gathering systems

Additional options are available when designing gathering systems for double-flash power plants due to the usage of the separated liquid at the power station. The four main configurations are;

- **High and low pressure separators at each wellhead** with high and low pressure steam pipes to the powerhouse and water pipelines to the injection wells.
- **Satellite system of High and low pressure steam separators in the field** with high pressure and low pressure steam pipelines to the powerhouse and water pipes to injection wells.
- **Satellite system of high pressure steam separators in the field** with water- and high pressure steam pipelines to the powerhouse, where the water enters a low pressure separator with a short steam pipe to the turbine and a water pipe to the injection well. This system is in use at Hellisheiði power plant.
- **System with common high and low pressure separators** Pipelines with Two-phase fluid lie to the powerhouse where the mixture is flashed twice. From the separators the steam flows to the turbine through short high and low pressure steam pipes to the turbines and a water pipe from the low pressure separator to the injection well (DiPippo 2007).

3.3.2 Plant components and thermodynamics

To describe the state of the geothermal fluid at each point in the working cycle, a thermodynamic state diagram, shown in Figure 3.5, is drawn, similar to the one used to describe the single-flash power plant.

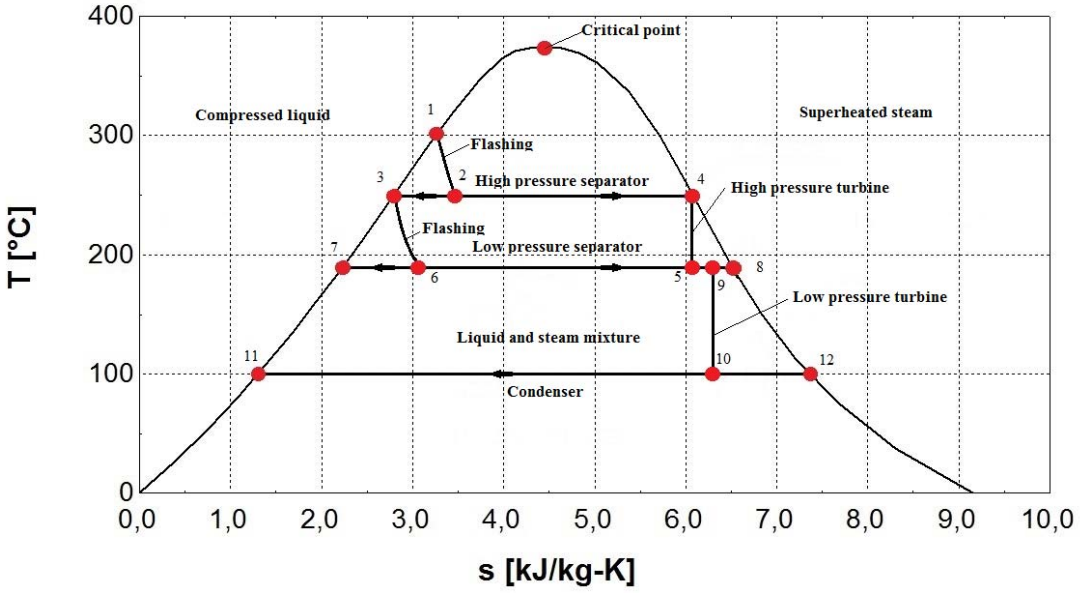

Figure 3.5 *s-T diagram for a double unit double-flash power plant*

The expansion process in the turbines in Figure 3.5 is assumed to be ideal. As in the single flash example, the flashing is assumed to be isenthalpic. So the following holds

$$h_1 = h_2 \qquad 3.25$$

$$x_2 = \frac{h_2 - h_3}{h_4 - h_3} \qquad 3.26$$

$$h_3 = h_6 \qquad 3.27$$

$$x_6 = \frac{h_3 - h_7}{h_8 - h_7}. \qquad 3.28$$

The mass flow of steam and liquid at different locations can be calculated, the mass flow of the high pressure steam is

$$\dot{m}_4 = \dot{m}_5 = x_2 \dot{m}_{total} \qquad 3.29$$

where $\dot{m}_{total}$ denotes the two phase mass flow into the high pressure separator.

Similarly, the mass flow of the high pressure liquid is

$$\dot{m}_3 = \dot{m}_6 = (1 - x_2)\dot{m}_{total}. \qquad 3.30$$

The low pressure steam is extracted from the high pressure liquid. The mass flow of the low pressure steam is therefore

$$\dot{m}_8 = (1 - x_2)x_6\dot{m}_{total} \qquad 3.31$$

and the low pressure liquid mass flow can be calculated

$$\dot{m}_7 = (1 - x_2)(1 - x_6)\dot{m}_{total}. \qquad 3.32$$

These mass flow equations are used to calculate the power generation from the turbines, the amount of water to be re-injected into the reservoir and the cooling needed (DiPippo 2007). For double unit power plants, such as Hellisheiði power plant, the analysis of each turbine is the same as the analysis of a turbine for a single-flash system described in section 3.2.3.

3.4 Hellisheiði power plant

Hellisheiði power plant is the world's largest geothermal power station. It is located at the southern part of the Hengill high temperature geothermal area, which lies on the plate boundaries between the North American and Eurasian tectonic plates on the western volcanic zone of Iceland, about 25 km east of Reykjavík. The area, seen in Figure 3.6, is characterized by its permeability and multiple fumaroles and hot springs at the surface (Gunnlaugsson and Gíslason 2005).

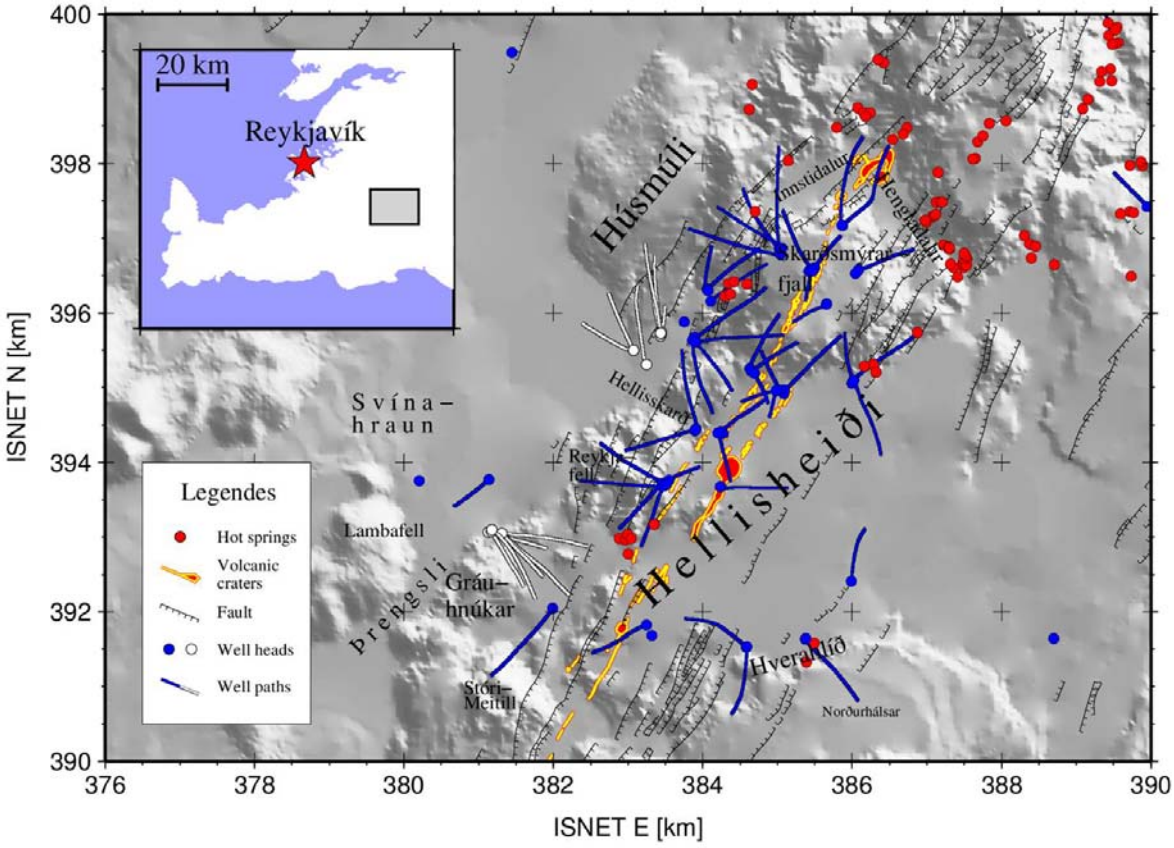

Figure 3.6 *Hellisheiði geothermal field (Gunnarsson 2013)*

The power plant started its operation in 2006. It utilizes geothermal fluid from the high temperature field Hengill to produce electricity and provide hot water to the Reykjavík area. Installed capacity is 133 MW thermal and 303 MW electric, consisting of six high pressure units generating 45 MW each and a single low pressure unit generating 33 MW. The reservoir is water dominated with an average enthalpy of 1750 kJ/kg (Gunnarsson 2013).

A two-phase mixture of steam and water is extracted from the production wells and is separated at the separation station. The 550 l/s of hot water that exits the separators when the power plant is operating at maximum capacity, is used to heat groundwater for district heating. The hot water is then re-injected into the reservoir at two reinjection sites (to maintain the reservoir's productivity) along with around 500 l/s of water that is condensed after exiting the power plants turbines. The substantial reinjection has induced seismicity and triggered earthquakes in the region (Bessason, Ólafsson et al. 2012, Gunnarsson 2013).

3.4.1 Assumptions

A number of assumptions are made to simplify the modeling of the power plant.

- It is assumed that no scaling forms at the inner walls of pipes at any point in the power plants working cycle.
- The process undergone by the fluid from the well to the separator is assumed to be isenthalpic.
- The processes in the steam separator and condenser are assumed to be isobaric.
- Pressure drop in smaller components and pipelines is neglected.
- Each 45 MW turbine has its own steam separator but since the pressure and mass flow of geothermal fluid at each separator inlet are not logged, the state of the fluid at the high pressure separator outlet is the starting point of the modeling.
- It is assumed that no steam exits the condenser via extraction of non-condensable gases.
- The data logged for the mass flow and pressure at the steam separator outlet, the condenser pressure and most importantly, the electric power output are assumed to be correct and are used as input parameters in the model calculations.

4 Modeling methods

To achieve the objectives listen in the introduction, a simple thermodynamic model of a single flash geothermal power plant is constructed. A schematic of the model is seen in Figure 4.1.

The model input variables are the average values of data collected at Hellisheiði over a two month period in early 2014 for the separator outlet pressure P_2, steam mass flow $\dot{m}_2$ and condenser pressure P_3, as well as a guessed value for the turbines base efficiency η_0. The base efficiency is a parameter used in geothermal power plant modeling, to estimate the unknown conditions at a turbine outlet based on the condenser pressure and the known conditions at the turbine inlet.

From the input variables, the model calculates the conditions at the turbine outlet, namely the steam quality x_3, and enthalpy h_3, using the Baumann rule described in Equations 3.11-3.16. Values for the isentropic efficiency η_s, provided by the turbine manufacturer and the total efficiency η, provided by Mannvit Engineering, are used to calculate the combined mechanical and generator efficiency $\eta_{m,g}$.

The isentropic efficiency and isentropic power output $\dot{W}_s$, are calculated from Equation 3.8, using the estimated conditions at the turbine inlet and outlet, i.e. the enthalpy at the turbine outlet according to the Baumann rule. The electric power output is then calculated, using the combined mechanical and generator efficiency and the calculated isentropic power output and isentropic efficiency.

The base efficiency is then changed in an iterative manner until the calculated electric power output matches the value logged at Hellisheiði. Since the isentropic and total efficiencies are dependent on the base efficiency, the iteration process results in different values for the total- and isentropic efficiencies than the ones provided by Mannvit Engineering and the turbine manufacturer respectively.

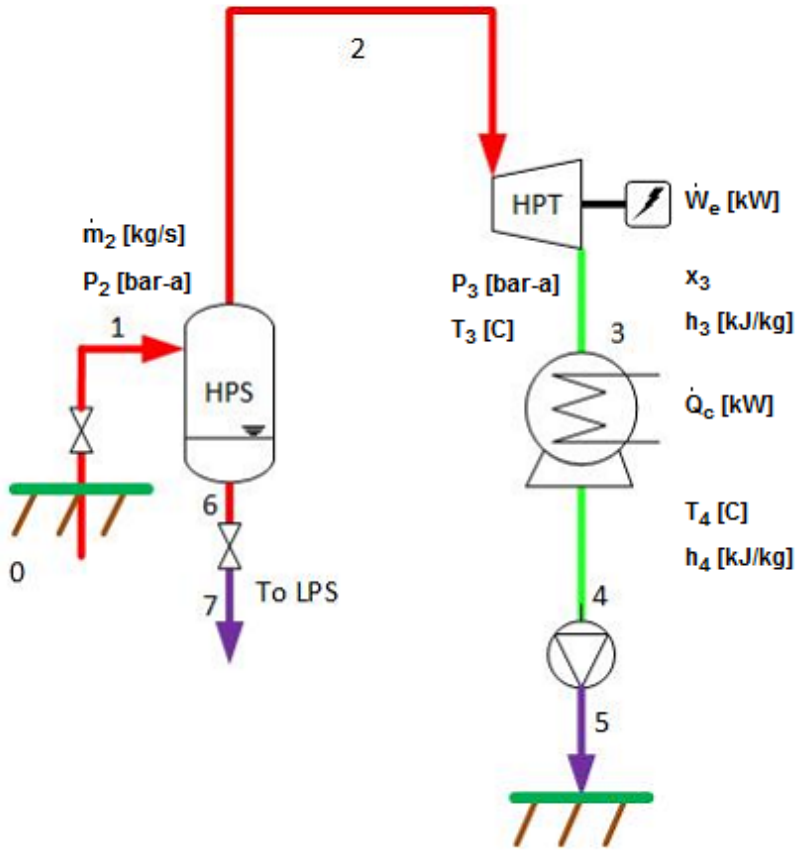

Figure 4.1 *Simple thermodynamic model of a single flash cycle*

The pressure is logged at both separator outlet and turbine inlet. Thus, the effects of excluding the pressure drop between the steam separator and the turbine on various parameters can be calculated by changing the input pressure of the model to turbine inlet pressure instead of separator outlet pressure.

Non-condensable gases are a small portion of the steam flow and generally neglected in simple models. To see what effect excluding them from the calculations has, the model is modified with an additional imaginary gas turbine, with the same specifications and parallel to the steam turbine. The non-condensable gas mass flow is subtracted from the steam flow and is assumed to pass through the imaginary gas turbine instead. Since the gas does not condense, the calculations for the imaginary gas turbine do not require the use of the Baumann rule. Summing the electric power output of the two turbines, results in the total electric power output.

The mass flow of all the cooling water that enters and leaves the condenser is logged as well as the temperature at all inlets and outlets. To verify the calculated steam quality and enthalpy at the turbine outlet, a thermodynamic model of the condenser is constructed (see Figure 6.3). The model's input variables are the average values of condenser pressure P_3, control valve opening ratios o_{12} and o_{15}, as well as the mass flow, temperature and pressure of all the condensers cooling water inlets and outlets. The model calculates the

energy received by the cooling water when it passes through each of condensers three steps. The total energy received along with the enthalpy at the condenser condensate outlet is then used to calculate the enthalpy at the turbine outlet using Equation 3.17.

The condenser model is also used to estimate the overall heat transfer coefficient of the condenser U. The specifications of the condenser used to calculate area of heat exchange A, is provided by Mannvit Engineering. From the Area of heat exchange and the temperature and mass flows logged, the model calculates the overall heat transfer coefficient using equations 3.17 to 3.24

5 Data gathering

The data used from Hellisheiði power plant was logged every hour over a roughly two month period in early 2014. The distribution of the data over time can be seen in Appendix A. The plots in the appendix show all the data available with the exception of a handful of measurements which were far off realistic values, most likely due to logger errors.

The data is quite stable from 26th of February onwards (see Appendix A). Before that time, the power plant seems to have been run under abnormal circumstances and thus, the data before that time is excluded. The average value over this time is used in the calculations. The standard error relative to the average value is calculated for every dataset and as seen from Table 5.1 the error is generally below 0.1%. Even though the error is low, the data might well be shifted, causing inaccuracy, for instance due to poor calibration of sensors.

The data for the groundwater flow rate $\dot{v}_8$, and groundwater temperature at condenser outlet T_9, show considerable variations in the preheating process for hot water production, as seen in Figure 5.1 and Figure 5.2 respectively. The model uses the average outlet temperature to calculate the overall heat exchanger effectiveness from equation 3.18. Thus, the overall heat coefficient calculated from the heat exchanger effectiveness might have somewhat higher error limits.

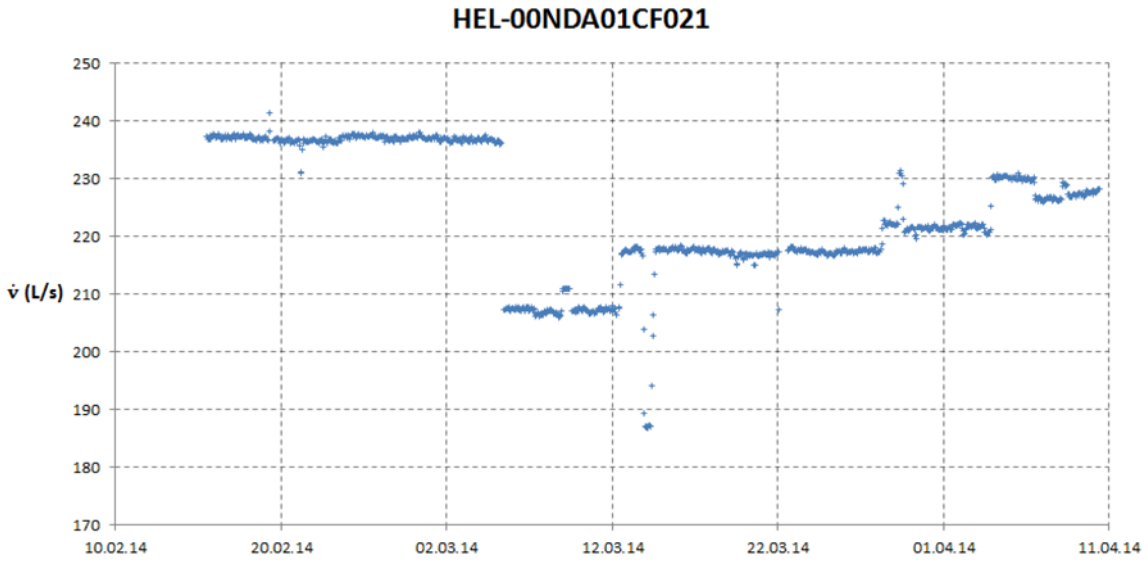

Figure 5.1 *Hellisheiði Unit 2 Condenser first step: groundwater flow rate*

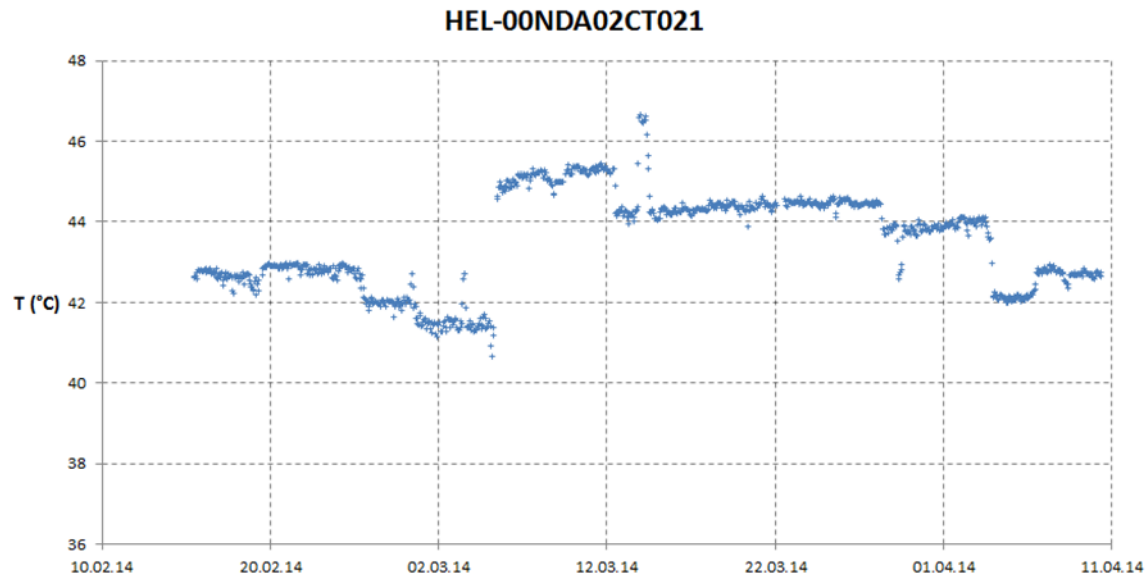

Figure 5.2 *Hellisheiði Unit 2 Condenser first step: groundwater outlet temperature*

Even though the data in Figure 5.1 and Figure 5.2 is somewhat unstable, a combination of the two measurements is used when calculating the energy transfer. Thus, the energy transfer plotted in Figure 5.3 is relatively stable.

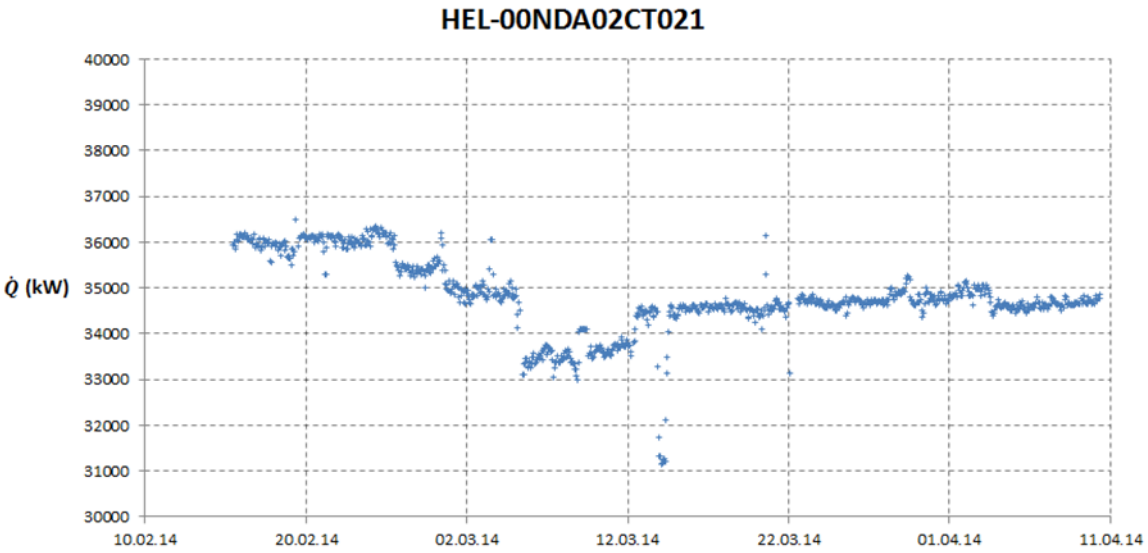

Figure 5.3 *Hellisheiði Unit 2 Condenser first step: energy transfer*

The flow rate of condensate out of the condenser is logged, and could be used to estimate the mass flow exiting the condenser via non-condensable gas extraction. The data for the condensate flow rate at the condenser outlet is unusable, since it is 75% higher than the flow of steam entering the condenser. This offset could be due to heavy leakage of cooling water into the condensing chamber, but the leakage would show in other data, which is not the case. The most probable explanation is that the logger is out of order, and thus, the data will not be used.

The average values along with the standard deviation, standard error and the standard error percentage of the measurements from 26th of February onwards, can be seen in Table 5.1, where the standard error percentage is the standard error relative to the average value.

Table 5.1 *Measurements at Hellisheiði power plant unit 2*

Measurement name	**Average value**	**Std. deviation**	**Std. error**	**Std. error (%)**
P_2: Separator outlet pressure (bar-a)	8.49	0.027	0.001	0.01
$\dot{v}_6$: Separator outlet water flow (l/s)	61.65	0.582	0.018	0.029
$\dot{m}_2$: Turbine inlet steam flow (kg/s)	83.84	0.290	0.009	0.011
$P_{2,2}$: Turbine inlet pressure (bar-a)	8.37	0.028	0.001	0.010
T_2: Turbine inlet temperature (°C)	171.89	0.157	0.005	0.003
Turbine rotation speed (RPM)	2992	1.690	0.052	0.002
$\dot{W}_e$: Electric power production (MW)	44.28	0.053	0.002	0.004
T_3: Turbine outlet temperature (°C)	51.45	0,388	0.012	0.023
T_3: Condenser pressure (bar-a)	0.115	0.002	0.000	0.057
$\dot{v}_8$: Water flow rate at condenser inlet step 1 (l/s)	221	10.055	0.309	0.140
T_8: Water temperature at condenser inlet step 1 (°C)	4.15	0.104	0.003	0.077
T_9: Water temperature at condenser outlet step 1 (°C)	43.69	1.258	0.039	0.088
T_{11}: Water temperature at condenser outlet step 2 (°C)	38.06	0.278	0.009	0.022
T_{14}: Water temperature at condenser outlet step 3 (°C)	33.77	0.314	0.010	0.029
$\dot{v}_{17}$: Water flow rate from cooling tower (l/s)	2036	12.745	0.392	0.019
T_{17}: Water temperature from cooling tower (°C)	19.02	0.270	0.008	0.044
o_{12}: Control valve opening ratio step 2 (%)	99.1	3.908	0.120	0.121
o_{15}: Control valve opening ratio step 3(%)	97.31	12.831	0.394	0.405
T_4: Condensate temperature at condenser outlet (°C)	49.15	0.361	0.011	0.023

6 Results and discussion

The models presented in this section are designed to simulate Hellisheiði power plant working cycle. The models are constructed using Engineering Equation Solver (EES). Matlab and Microsoft Excel are used to handle the logged data and figures. The results of the simulation are shown in Table 6.1 below. The EES model that performs the calculations can be found in Appendix B.

Table 6.1 *Simulation results*

Variable name	**Value**
$T_{2,2,sat}$: Temperature of saturated steam at $P_{2,2}$ (°C)	172.3
η_0: Base efficiency	0.935
η: Total efficiency	0.786
η_s: Isentropic efficiency	0.83
$\eta_{m,g}$: Combined mechanical and generator efficiency	0.947
$\eta_{calculated}$: Calculated total efficiency	0.811
$\eta_{s,calculated}$: Calculated isentropic efficiency	0.857
$\eta_{m,g,calculated}$: Calculated combined mechanical and generator efficiency	0.947
$\dot{W}_s$: Isentropic power output (MW)	54.60
$\dot{W}_e$: Calculated electric power output (MW_e)	44.29
x_3: Calculated steam quality at turbine outlet	0.8427
h_3: Calculated enthalpy at turbine outlet (kJ/kg)	2213
T_3: Calculated temperature at turbine outlet (°C)	48.59
T_4: Calculated temperature at condenser outlet (°C)	48.59
$\dot{Q}_C$: Condenser heat transfer (MW_{th})	168.52

The conditions of the fluid at the steam separator inlet, point 1 in Figure 6.1, are not logged. Thus the models input values are mass flow $\dot{m}_2$ and pressure P_2 at the steam separator outlet point 2. Since the steam exiting the separator is very close to the saturation

point, the temperature T_2, entropy s_2, and enthalpy h_2, at the separator outlet can be calculated.

The pressure drops slightly in the pipes and components between the steam separator outlet and the turbine inlet, namely in the moisture remover. When constructing simple models to simulate a geothermal power plant, these pressure losses are usually neglected. The turbine inlet pressure and temperature are logged however, so the effects of not including this pressure drop can be estimated.

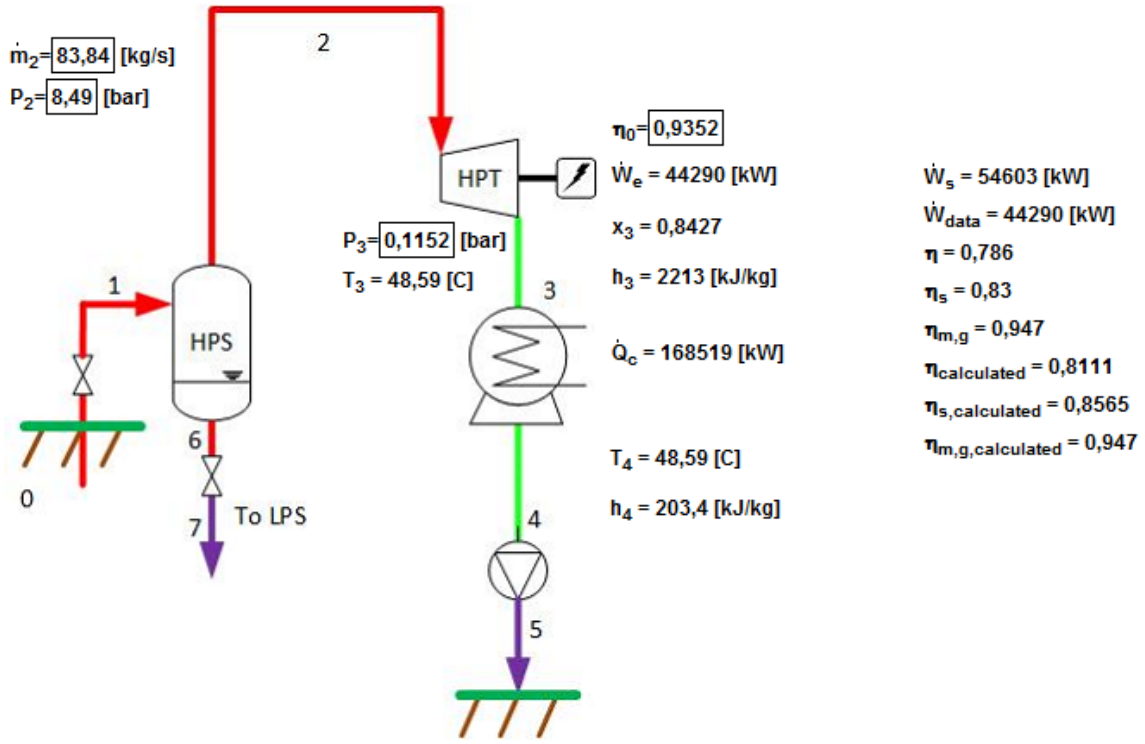

Figure 6.1 *Schematic of the simple single flash condensing power plant model*

In Figure 6.1, the colors of the lines represent different pressures, the red line denotes separator pressure, the green line denotes the condenser pressure and the purple line denotes intermediate pressure used for the bottom cycle and during re-injection.

6.1.1 Turbine efficiency

When calculating the power output of the turbine, two new input variables are needed, the condenser working pressure P_3, and the base efficiency of the turbine η_0, which is the efficiency of the turbine assuming the flow through it is dry steam (see Equation 3.11).

The steam quality x_3 and enthalpy h_3, at the turbine outlet, point 3 in Figure 6.1, are estimated from the Baumann rule as described in Equations 3.15 and 3.16. From the enthalpy, the power output can be calculated using Equation 3.6.

The total efficiency of the electricity generation η, is a product of the generator efficiency η_g, the mechanical efficiency η_m and the isentropic efficiency η_s. The manufacturer

provides values for the isentropic efficiency of the turbine and an estimated value for the total efficiency is provided by Mannvit Engineering (Harðarson and Ágústsson 2014). The isentropic power output can be calculated using equation 3.6 where no losses occur ($\dot{Q} = 0$), and where h_{out} is the isentropic enthalpy h_s at the turbine outlet. From the isentropic power output $\dot{W}_s$, the electric power output $\dot{W}_e$ becomes

$$\dot{W}_e = \dot{W}_s\eta = \dot{W}_s\eta_s\eta_m\eta_g. \qquad 6.1$$

The electric power output is logged at the power plant and the unknown factors of Equation 6.1 are the mechanical- and generator efficiencies. These efficiencies can be calculated as a combined mechanical- and generator efficiency $\eta_{m,g}$. The base efficiency of the turbine can now be found by iteration in such a way so that the calculated electric power output matches the electric power output logged. A value of 0.9 for a turbine base efficiency is often assumed when making simple models of geothermal power plants (Pálsson 2014). Here, the iterated value is 0.9352 or slightly higher than normally assumed, by about 3.7%.

Altering the base efficiency results in different values for both the isentropic efficiency and the total efficiency that are used to calculate the combined mechanical- and generator efficiency.

It is worth to note that the combined mechanical and generator efficiency calculated using the values η_s and η provided by the turbine manufacturer and Mannvit Engineering respectively, is almost identical to the combined mechanical and generator efficiency calculated from $\eta_{s,calculated}$, which is calculated using the turbine inlet and outlet enthalpies and $\eta_{calculated}$, which is calculated from the isentropic and total power generation. The error that appears by using the original values for η_s and η to determine the combined mechanical and generator efficiency is therefore negligible.

As seen from Table 6.1, the isentropic- and total efficiencies are somewhat higher than the values given by the manufacturer and Mannvit Engineering respectively. The base efficiency can also be iterated so that the calculated isentropic and total efficiencies match the values provided. This results in a base efficiency of 0.905. The consequence of this however, is lower electric power output than actually logged at the power plant, which is unlikely, since the logged electric power output is regarded as the most reliable parameter in the plant operation.

Despite the assumption that the pressure and mass flow at the separator outlet is correct and the standard error of the averages is quite low, these numbers might include some inaccuracy due to systematic shift, perhaps due to poor calibration. In order to examine this, model calculation can be done by fixing the base efficiency, so that the isentropic- and total efficiency match the provided values. As a result, the calculated electric power production is lower than the logged one. For the calculated electric power production to match the logged one, the pressure and/or mass flow at the steam separator outlet and the condenser pressure can be altered separately. In the case of the steam separator outlet pressure, the value of 9.9 bar-a is needed instead of 8.49 bar-a. Such a difference is regarded as unlikely. In the case of the mass flow, a value of 86.5 kg/s is needed instead of 83.84 kg/s. In the case of the condenser pressure, the needed pressure is 0.095 bar-a instead of the 0.1152 bar-a logged. It is considered unlikely that a single variable is the cause of

this difference. However, a combination of inaccuracies in the input parameters could cause such a difference.

The pressure is logged at both the separator outlet and the turbine inlet. The logged temperature at the turbine inlet seen in Table 5.1 is 0.46 °C lower than the saturation temperature of steam at the turbine inlet pressure, resulting in sub cooled liquid. The difference is less than the error of the temperature data. The temperature loggers are often not calibrated correctly and the data shift increases with time since last calibration. The pressure measurements are more reliable and should be used instead of the temperature measurements (Benediktsson and Einarsson 2014).

The calculated temperature at the turbine outlet T_3 in Table 6.1 is 2.86 °C lower than the logged temperature $T_{3,data}$, corresponding to 5.6% difference. It is calculated using the logged condenser pressure and the calculated enthalpy h_3, at the turbine outlet. The value of the calculated temperature is sensitive to condenser pressure changes. For the calculated temperature to match the logged one, the condenser pressure P_3 needs to be 13% higher than measured, i.e. 0.1328 bar-a instead of 0.1152 bar-a. Since the pressure measurements are generally more reliable (Benediktsson and Einarsson 2014), the error is likely caused by a poorly calibrated temperature logger.

6.1.2 Pressure drop between separator and turbine

Estimating the error of not including the pressure drop between steam separator and turbine is possible by using the turbine inlet pressure instead of the separator outlet pressure as an input into the model. The base efficiency is then altered again so that the calculated electric power output matches the logged electric power output.

Table 6.2 *Comparison of values when including pressure drop between separator and turbine*

Variable	**Value at P_2 = 8.49 bar-a (excluding pressure drop)**	**Value at P_2 = 8.37 bar-a (including pressure drop)**	**Change**
η_0	0.9352	0.9382	0.32%
$\eta_{calculated}$	0.8111	0.8138	0.33%
$\eta_{s,calculated}$	0.8565	0.8594	0.34%
$\dot{W}_s$	54.603 MW	54.423 MW	-0.33%
x_3	0.8427	0.8424	-0.04%
h_3	2213 kJ/kg	2213 kJ/kg	0.0%
$\dot{Q}_C$	168.52 MW	168.471 MW	-0.03%

The error caused by neglecting the pressure drop from separator to turbine is low and has no significant effects on the power generation model results.

6.1.3 Non Condensable Gas

The effect of non-condensable gases on the power production can be estimated by modeling an imaginary turbine with the same specifications as the actual turbine and assuming that all the non-condensable gas passes through the imaginary turbine. Combining the power generation of the two turbines and altering the base efficiency so that the combined power matches the power logged in the data, gives estimation for the change in the base efficiency. The change in base efficiency can then be used to see if excluding the non-condensable gases in the simple model is justified.

The gas consists of roughly 85% carbon dioxide and 15% hydrogen sulfide and the amount of gas in the total mass flow is usually around 0.5% (Sigurðardóttir, Gíslason et al. 2010). For simplicity, the gas is assumed to be carbon dioxide only. During a performance test of Hellisheiði unit 5 however, the gas content was observed to be 0,361% (Sakanaka and Ágústsson 2011). The comparison of the base efficiencies, when a NCG content of 0.361% is included in the calculations, can be seen in Table 6.3 below.

Table 6.3 *Comparison of base efficiency change when including non-condensable gases*

Variable	**Without NCG**	**With NCG**	**Change**
η_0	0.9352	0.9346	-0,07%
x_3	0.8427	0.8428	0.01%
h_3	2213 kJ/kg	2214 kJ/kg	0.05%
$\dot{Q}_c$	168.52 MW	168.55 MW	0.02%
$\dot{W}_e$	44.29 MW	44.29 MW	0%

As expected, the base efficiency necessary to maintain constant power output decreases slightly when non-condensable gases are taken into account. The change is minimal however, thus neglecting the non-condensable gases in the case of Hellisheiði power plant is reasonable. These estimations do not apply to power plants with high non condensable gas content however.

The change in necessary base efficiency for increased non-condensable gas content at constant power production can be seen in Figure 6.2 below.

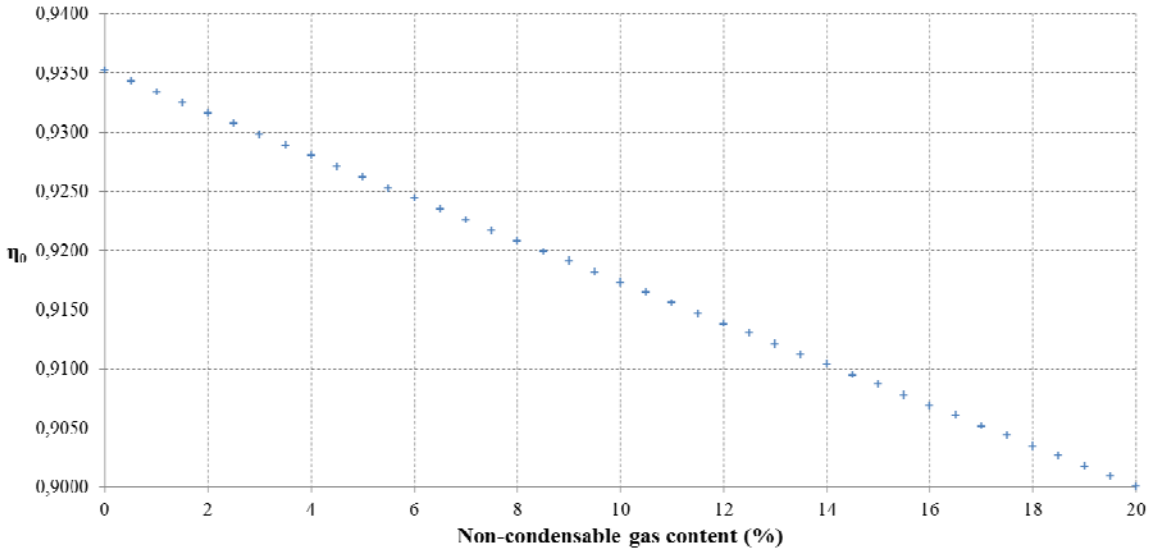

Figure 6.2 *Change in base efficiency with increased NCG flow at constant power output*

As seen in Figure 6.2, the necessary base efficiency to maintain constant power output decreases linearly with increased non-condensable gas content in the steam. Higher gas content increases the turbines production, but also increases the power and cost associated with gas extraction in the condenser (Dickson and Fanelli 2003).

6.1.4 Condenser

The condenser at Hellisheiði power plant, shown in Figure 6.3, is a closed type condenser and consists of three steps. The first step is at the top of the condenser where cold groundwater flows in at point 8, is pre-heated by the condensing steam to be used for district heating. Non-condensable gases are extracted from the condenser using liquid ring vacuum pumps (Harðarson and Ágústsson 2014). The mass flow reduction due to non-condensable gases is accounted for in the calculations. The next two steps consist of circulating water from the cooling towers entering the condenser at points 12 and 15 and exiting at points 11 and 14 respectively.

By assuming constant pressure in the condenser and that all the steam entering it is condensed into liquid, the temperature T_4, enthalpy h_4 and entropy s_4 at the condenser outlet, point 4, can be calculated, from which the energy removed from the condensate $\dot{Q}_C$ can be derived.

Energy transfer

To verify the steam quality and enthalpy at the turbine outlet as well as the calculated energy transfer of the condenser a thermodynamic model which focuses on the cold end of the condenser is constructed. Temperature differences and flow of cooling water through the condenser are logged and can be used to estimate the energy transfer from the condensate to the cooling fluid. From the energy transfer, the inlet enthalpy and quality of the steam can be evaluated and compared with the values calculated using the Baumann rule in the model shown in Figure 6.1. In the cold end model, the mass flow into the condenser is assumed to contain 0.361% non-condensable gases that are extracted from the steam in the condenser and it is assumed that no steam exits the condenser via gas

extraction. Furthermore, it is assumed that no heat is lost to the environment and that the pressure at all cold end inlets and outlets is constant at 1.9 bar-a. A schematic of the cold end model is shown in Figure 6.3.

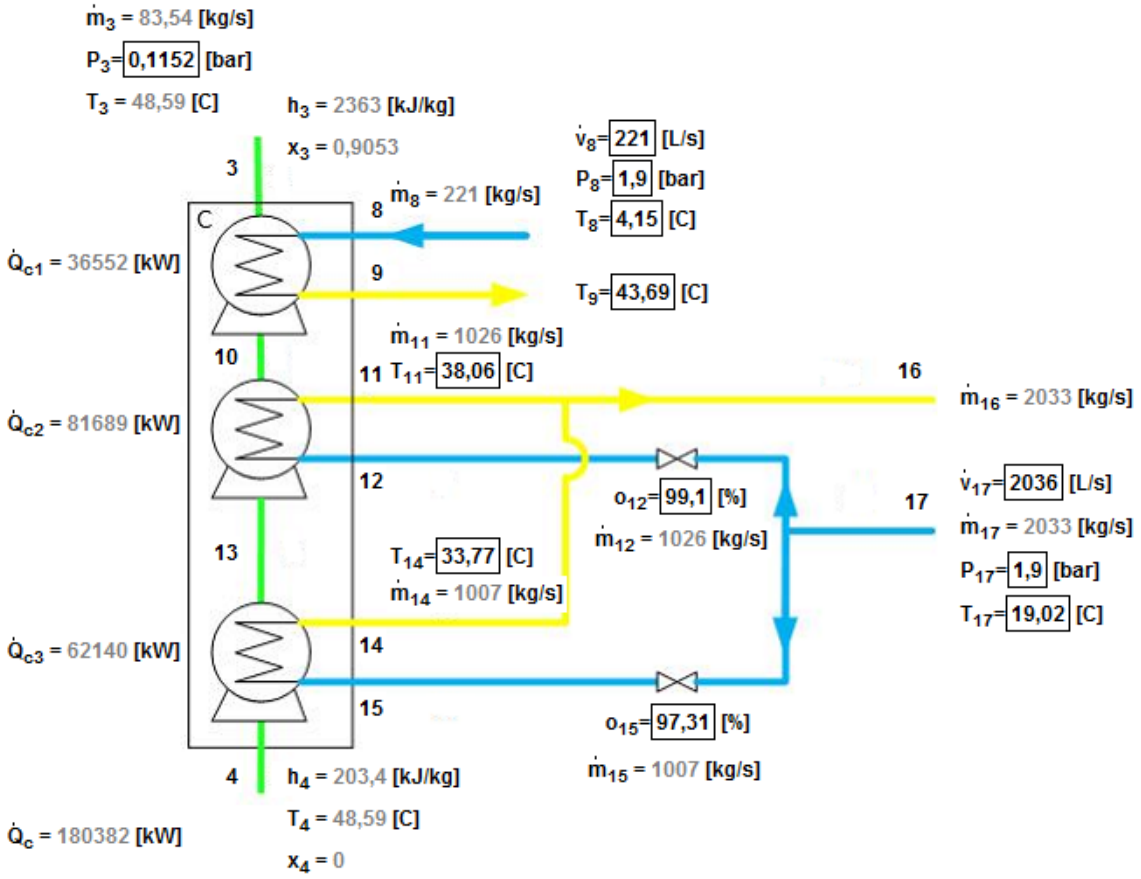

Figure 6.3 *Condenser energy transfer model*

The green lines in Figure 6.3 denote the steam passing through the condenser at the condenser pressure. The blue and yellow lines represent cold and warm cooling water respectively. The input variables are marked by box around them and contain average values of data from Hellisheiði power plant.

The calculated heat transfer $\dot{Q}_C$, the steam quality x_3, and the enthalpy h_3, at the turbine outlet, are considerably higher than the calculated values shown in Table 6.3. The energy received by the colder fluid in a heat exchanger can of course never be higher than the energy donated by the hotter fluid. The temperature measurements of the cold end have no significant value to the power plant operators since they do not affect the power production and can easily be a few degrees off without it being noticed (Benediktsson and Einarsson 2014).

The calculated condensate temperature at the condenser outlet T_4 in Table 6.1 is 1.1% lower than the logged temperature $T_{4,data}$. To get a better view of what that means, the two temperatures are plotted on a T-s diagram shown in Figure 6.4 below.

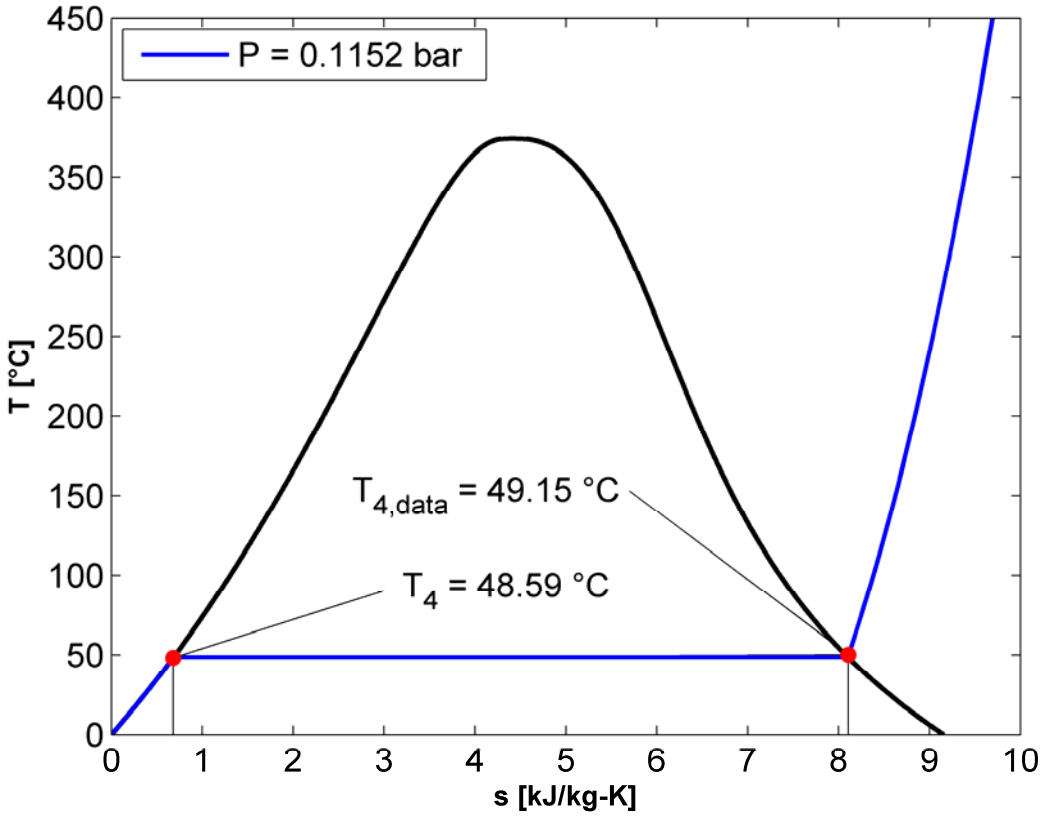

Figure 6.4 *Comparison of calculated and logged temperature at condenser outlet*

As seen on Figure 6.4, the logged condenser outlet temperature at the logged condenser outlet pressure results in saturated steam, which is clearly not the case, since the condenser condenses the steam. The actual temperature is most likely lower than the logged value, since pressure measurements are more reliable and the water in the condenser generally cools by a few degrees after condensation. The process is not completely isobaric and the pressure might have changed slightly from where the pressure is logged to the condenser outlet where the temperature is logged. As an example, for the fluid to be in liquid state at the logged condenser outlet temperature, the pressure would need to be only 0.003 bar-a higher. The measurement error, whether it lies in potential pressure increase in the condenser or in the temperature logged, is small.

Since most of the cooling water flowing through the condenser comes from the cooling tower, the model is especially sensitive to changing temperature of cooling water from the cooling tower T_{17}. For the heat received by the cooling water to match the heat donated by the condensate as calculated in the model shown in Table 6.3, the temperature of cooling water from the cooling tower needs to be 1.4 °C higher than measured. The error is most likely due to poor maintenance of the cold end temperature loggers, causing them to consistently show lower values. Using a cold end model to verify the calculated values of the condenser inlet enthalpy and steam quality from Table 6.3 is therefore not feasible.

Overall heat transfer coefficient

The cold end model seen in Figure 6.3 calculates the condenser effectiveness ϵ, the overall heat transfer coefficient U, and the number of transfer units N, using equations 3.17 through 3.24.

The area of heat exchange A, shown in Table 6.4, is calculated from the condenser specifications provided by Mannvit Engineering, namely pipe diameters, lengths and number of pipes. The bottom row shows the calculated value for the overall heat transfer coefficient, once the temperature of the cooling water from the cooling tower has been raised by 1.4 °C to account for the error in energy transfer.

Table 6.4 *Condenser pipes and area of exchange specifications (Harðarson and Ágústsson 2014)*

	Condenser step 1, district heating	**Condenser step 2, circulation from cooling tower**	**Condenser step 3, circulation from cooling tower**
Pipe material	Titanium	Titanium	Titanium
Pipe diameter (mm)	19	23	23
Pipe length (mm)	10630	10630	10630
Number of pipes	4373	2015	3120
Calculated area of heat exchange (m^2)	2775	1548	2396
Calculated overall heat transfer coefficient (W/m^2K)	734.8	2728	1130

To estimate one single overall heat transfer coefficient for the entire condenser, it must be altered to have only one cooling water inlet and one cooling water outlet. The model calculates the energy content of the cooling liquid at each inlet and outlet with absolute zero (0 K) as reference temperature. Summing the energy of the inlets/outlets, results in the energy of the cooling fluid if it were mixed to flow through a single inlet/outlet. From the energy, the model calculates the combined inlet and outlet temperatures and finally, calculates the overall heat transfer coefficient for the entire condenser, using the same method as for each condenser step. The calculated overall heat transfer coefficient for the entire condenser is 1288 W/m^2K. Performed calculations can be seen in the cold end model calculations in Appendix B.

The value of the overall heat transfer coefficient for steam condensers varies, usually within the range 1100-5600 $W/m^2°C$ for (Holman 2010). A value of 2000 W/m^2K is typically used for steam-water heat exchanger calculations for geothermal power plants (Karlsdóttir 2008).

7 Conclusions

The objective of this thesis was to examine to what extent simple thermodynamic models can be used to simulate the working cycle of an operating geothermal power plant. To achieve this, a simple thermodynamic model of a single flash geothermal power plant was constructed and its results compared to data from a high pressure single flash unit at Hellisheiði power plant.

The base efficiency of a turbine is an important input parameter for simple thermodynamic models, since the steam conditions at the turbine outlet, calculated using the Baumann rule, are derived from it. Turbine manufacturers normally do not provide values for the base efficiency and thus it must be estimated. A reasonable value for the turbine's base efficiency was found by fixing the power generation in the model to match the power generation logged. The acquired value for the base efficiency was observed to be slightly higher than values commonly used when modeling geothermal power plants.

If the data used as input parameters in the model are correct, the resulting isentropic and total efficiency are higher than the provided values. It was calculated that 15-20% inaccuracy in either of the models input pressure values or a 3% inaccuracy in the input mass flow could cause this deviation. It is highly unlikely however, that such systematic inaccuracies are present in the pressure data.

Neglecting the pressure drop through pipes and components between the steam separator and the turbine, were found to have minimal effects on the efficiencies and the steam conditions at the turbine outlet.

A performance test conducted at Hellisheiði power plant shows the amount of non-condensable gases present in the turbine steam flow. Including these gases in the turbine calculations had little to no effect on the turbines base efficiency and steam conditions at the turbine outlet. The change in base efficiency needed to maintain constant power output with increasing non-condensable gas content was plotted in Figure 6.2. The results provide an idea of at when the non-condensable gases need to be included in the calculations and the resulting change in the base efficiency.

The steam conditions at the turbine outlet, calculated using the Baumann rule, investigated using a model of the condensers cold end. The unreliability of the temperature loggers prevented accurate calculations of the energy transfer and thus the steam conditions at the turbine outlet could not be verified. However the calculated steam conditions at the turbine outlet can be used to estimate the error in the condenser temperature loggers.

The overall heat transfer coefficient for both the condensers individual steps and the condenser as a whole was estimated using the NTU method. The values for the individual steps varied and were found to be mostly in the lower part of the typical range for steam condensers. The value for the entire condenser was found to be 1288 W/m^2K, about 36% lower than a typical value for a condenser of a geothermal power plant.

The results above can serve as a guide when constructing simple models to simulate geothermal power plants. Namely to give an idea of

- what value to use for the base efficiency of a turbine
- whether or not pressure drop calculations between separator and turbine are needed
- when it is necessary to include non-condensable gas calculations for the turbine
- the type of a gas extraction system needed, based on the gas content in the steam
- the cooling capacity needed in the condenser
- the condensers effectiveness and its overall heat transfer coefficient

7.1 Further studies

When modeling geothermal power plants, the properties of the geothermal fluid at the reservoir is often the only data available. It would therefore be useful to know the pressure drop and the flow type of the two-phase fluid up the well and in the pipelines from the well to the steam separator.

The separation process is often modeled as an isobaric process. As stated before, that is not the case. Researching the actual pressure drop across various steam separators for different fluid properties would be useful for designers of geothermal power plants.

It would be useful to develop a summary of mechanical and generator efficiencies for different turbines and finding estimated values for those efficiencies for simple power plant models.

Furthermore, researching the accuracy of the Baumann rule by measuring the steam conditions at the turbine outlet would be a worthy addition. This could also be done by estimating the heat lost to the environment in the condenser and using reliable data for its cold end, to estimate the conditions at the turbine outlet. If the conditions at the turbine outlet are measured, the heat loss in the condenser to the environment could also be estimated, if reliable data for its cold end is available.

References

Arriaga, M.-C. S. (2005). *A Short Story of the Long Relationship Between The Human Race and Geothermal Phenomena*. World Geothermal Congress, Antalya, Turkey, School of Physics & Mathematical Sciences, Ed. B, Michoacan University.

Benediktsson, D. Ö. and Ó. P. Einarsson (2014). Discussion on temperature measurements at geothermal powerplants.

Bertani, R. (2010). *Geothermal Power Generation in the World 2005–2010 Update Report*. World Geothermal Congress. Bali, Indonesia.

Bertani, R. (2014). *Geothermal Power Generation in the World 2010-2015 Update Report*. Submitted to World Geothermal Congress 2015. Melbourne, Australia, International Geothermal Association.

Bertani, R. and J. W. Lund (2010). *Worldwide Geothermal Utilization 2010*. USA.

Bessason, B., E. H. Ólafsson, G. Gunnarsson, Ó. G. Flóvenz, S. S. Jakobsdóttir, S. Björnsson and Þ. Árnadóttir (2012). *Verklag vegna örvaðrar skjálftavirkni í jarðhitakerfum*. Reykjavík, Orkuveita Reykjavíkur.

Dickson, M. H. and M. Fanelli (2003). *Geothermal Energy, Utilization and technology*. Paris, France, UNESCO publishing.

Dickson, M. H. and M. Fanelli. (2004). *"What is Geothermal Energy?"*, 2004, from http://www.geothermal-energy.org/geothermal_energy/what_is_geothermal_energy.html.

DiPippo, R. (2007). *Geothermal Power Plants, Principles, Applications, Case Studies and Environmental Impact*, BH.

Flóvenz, Ó. G. (2012). *General aspects of geothermal energy*. I. Geosurvey. Iceland, University of Iceland.

Flóvenz, Ó. G. (2014). Discussion on geothermal energy.

Gunnarsson, G. (2013). Hellisheidi geothermal field. Reykjavík, Reykjavík Energy.

Gunnarsson, G. (2013). Temperature Dependent Injectivity and Induced Seismicity. Managing Reinjection in the Hellisheiði Field, SW-Iceland. Reykjavík, Reykjavik Energy.

Gunnarsson, G. (2013). "Temperature Dependent Injectivity and Induced Seismicity - Managing Reinjection in the Hellisheiði Field, SW-Iceland." GRC Transactions **37**.

Gunnlaugsson, E. and G. Gíslason (2005). *Preparation for a New Power Plant in the Hengill Geothermal Area, Iceland*. World Geothermal Congress. Antalya, Turkey, Reykjavik Energy.

Harðarson, F. and G. Ó. Ágústsson (2014). Discussion regarding the working cycle of Hellisheiði power plant.

Holman, J. P. (2010). *Heat Transfer*, McGraw-Hill.

Jóhannesson, Þ. (2012). Discussion on pressure drop accross steam separators.

Jóhannesson, Þ. and Y. Guðmundsson (2012). *Mechanical design of geothermal power plants - cold end (Cooling towers)*. Lecture notes in the course Geothermal Power Plants, University of Iceland.

Jóhannesson, Þ. and Y. Guðmundsson (2012). *Mechanical Design of Geothermal Power Plants - Condenser and Non-Condensable Gas Extraction*. Lecture notes in the course Geothermal Power Plants, University of Iceland.

Jóhannesson, Þ. and Y. Guðmundsson (2012). *Mechanical Design of Geothermal Power Plants - Drilling & Gathering Systems*. Lecture notes in the course Geothermal Power Plants, University of Iceland.

Karlsdóttir, M. R. (2008). *Utilization of Geothermal brine for Electrical Power Production* M.sc, University of Iceland.

Landsvirkjun. (2013). *"Þeistareykir."* Retrieved 2014.7.14, 2014, from http://www.landsvirkjun.is/rannsoknirogthroun/virkjunarkostir/theistareykir.

Lund, J. W. (2006). *History, present utilization and future prospects of geothermal energy worldwide*. Oregon, United States of America, Oregon Institute of Technology.

Mannvit. (2011). *"Bjarnaflag Geothermal Power Plant (2011 - ongoing)."* Retrieved 2014.7.9, 2014, from http://www.mannvit.com/GeothermalEnergy/ProjectExampleinfo/bjarnaflag-geothermal-power-plant-2011--ongoing.

Pálmason, G. (2005). *Jarðhitabók Eðli og nýting auðlindar*. Reykjavík, Hið íslenska bókmenntafélag.

Pálsson, H. (2012). *Overview of geothermal power plants in Iceland*. Lecture notes in the course Geothermal Power Plants, University of Iceland.

Pálsson, H. (2012). *Utilization of geothermal energy for power production* - Lecture notes. Iceland, University of Iceland.

Pálsson, H. (2014). Discussion on simple thermodynamic models.

Ragnarsson, Á. (2010). *Geothermal Development in Iceland 2005-2009*. World Geothermal Congress. Bali, Indonesia.

Sakanaka, Y. and G. Ó. Ágústsson (2011). *Turbine Performance Test Report (Unit 5)*. L. Mitsubishi Heavy Industries.

Sigurðardóttir, H., S. R. Gíslason, W. S. Broecker, E. H. Oelkers and E. Gunnlaugsson (2010). *The CO2 Fixation into Basalt at Hellisheiði Geothermal Power Plant, Iceland*. World Geothermal Congress. Bali, Indonesia.

Trinnaman, J. and A. Clarke (2010). *2010 Survey of Energy Resources*, World Energy Council.

Appendix A

The following figures show data logged at Hellisheiði power plant from the 15th of February 2014 to the 10th of April 2014.

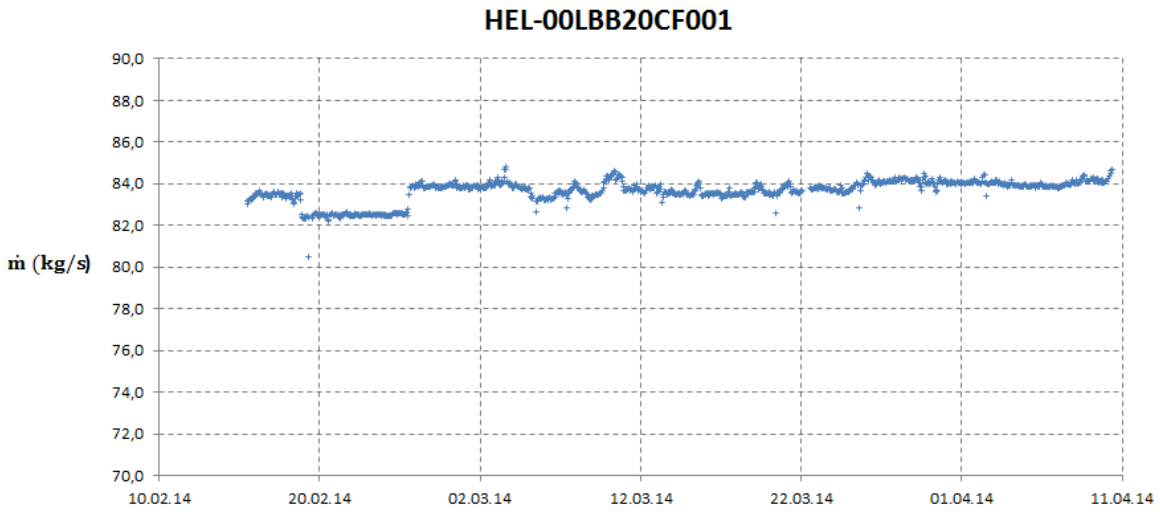

Figure A.1 *Hellisheiði Unit 2 Turbine inlet steam flow*

The data seen in Figure A.1 is relatively stable. Some sudden offsets appear before the 26th of February.

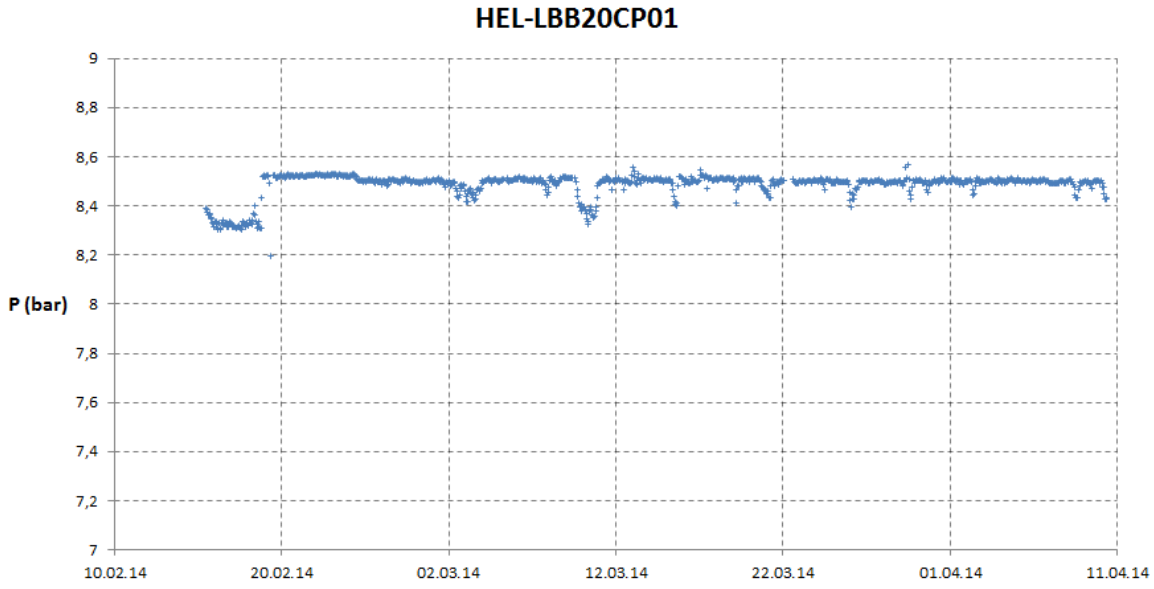

Figure A.2 *Hellisheiði Unit 2 Pressure at steam separator outlet*

The data seen in Figure A.2, Figure A.3 and Figure A.4 is stable, except for an offset proceeding February the 19th.

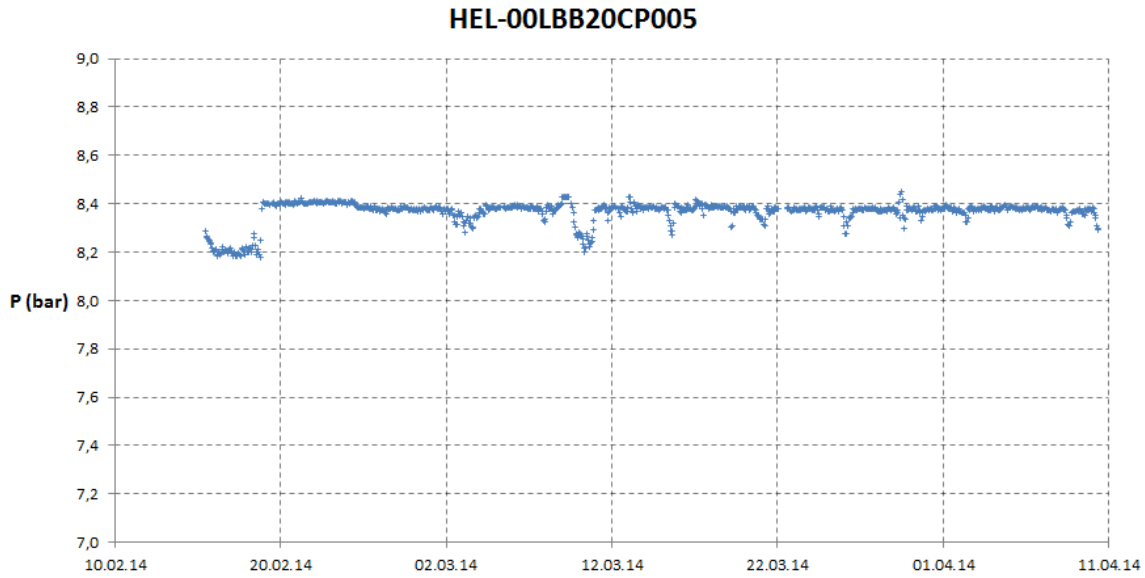

Figure A.3 *Hellisheiði Unit 2 Turbine inlet pressure*

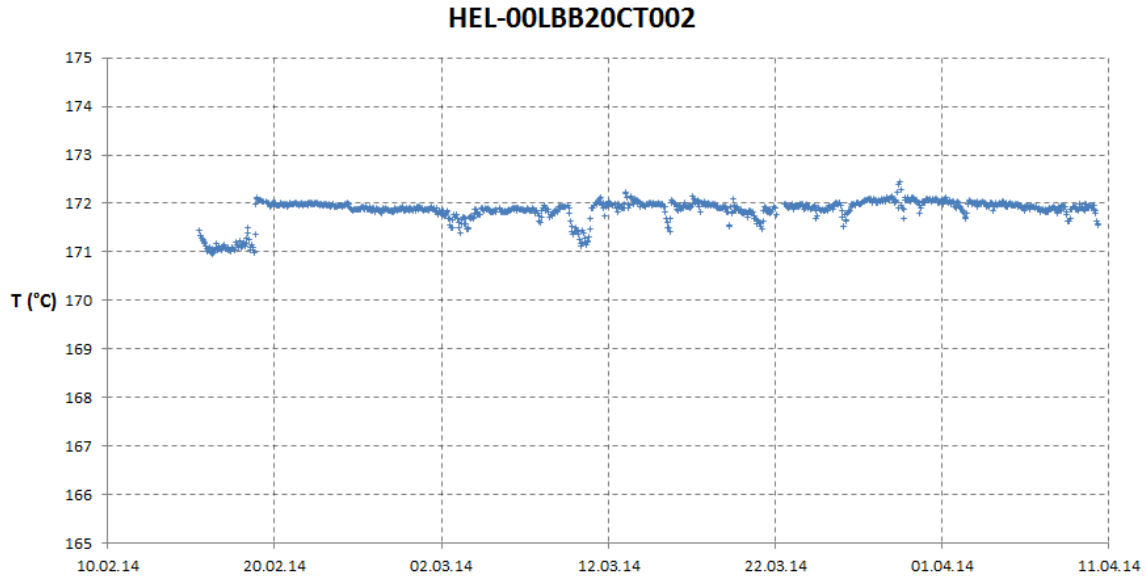

Figure A.4 *Hellisheiði Unit 2 Turbine inlet temperature*

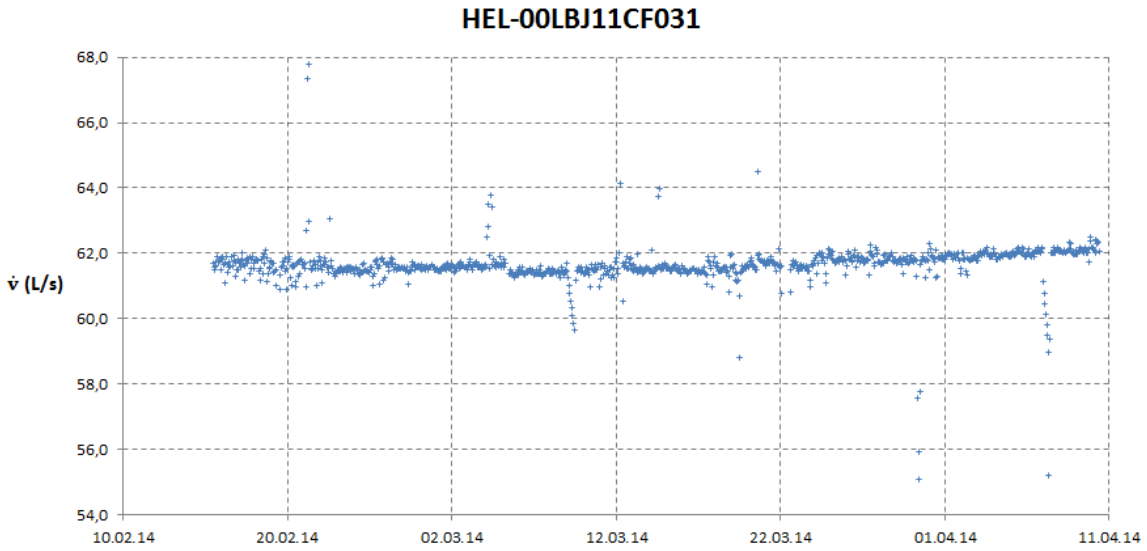

Figure A.5 *Hellisheiði Unit 2 Water flow at steam separator outlet*

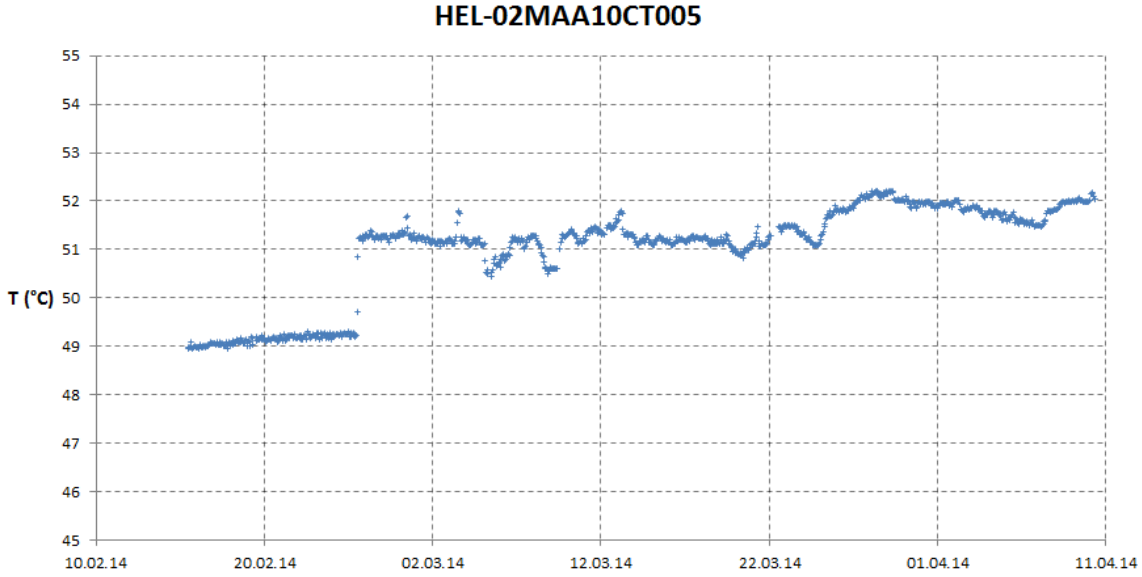

Figure A.6 *Hellisheiði Unit 2 Turbine outlet temperature*

Turbine outlet temperature data shown in Figure A.6 is relatively stable after February the 26th.

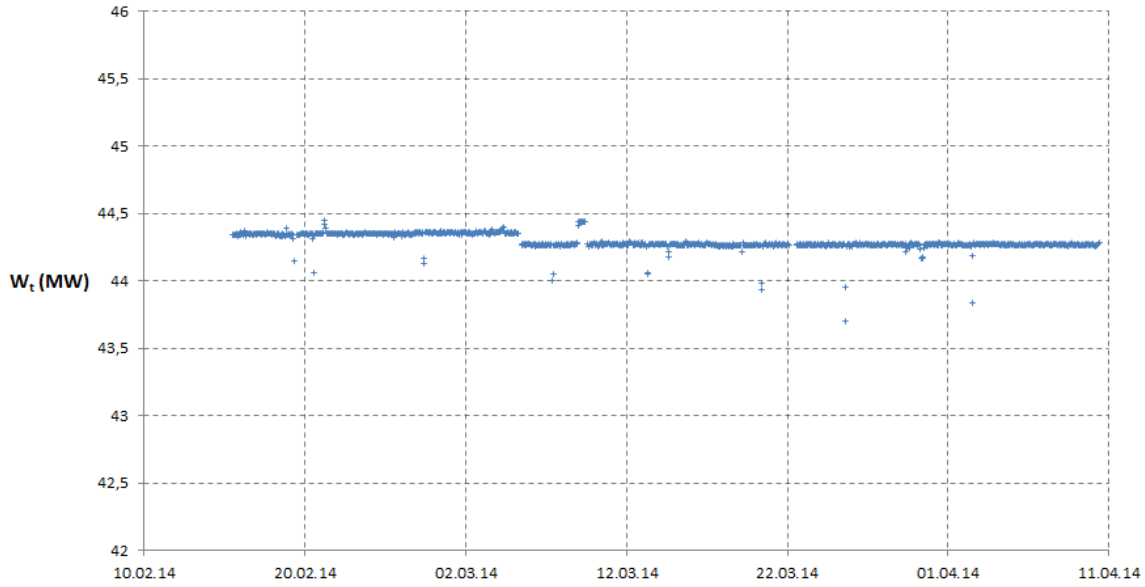

Figure A.7 *Hellisheiði Unit 2 Turbine power output*

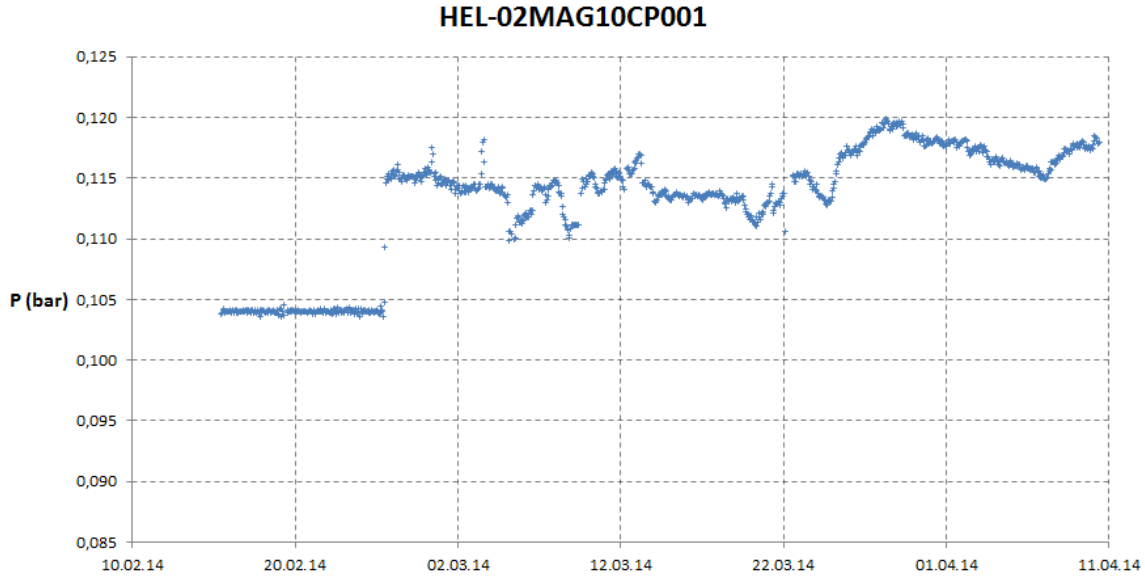

Figure A.8 *Hellisheiði Unit 2 Condenser pressure*

Condenser pressure data shown in Figure A.8 is stable after February the 26th.

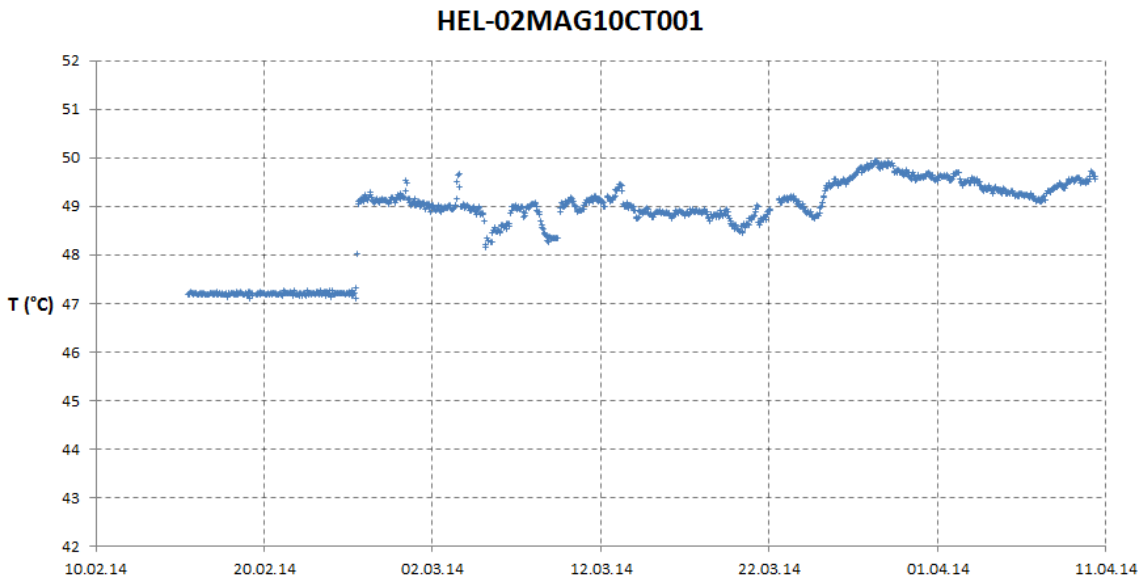

Figure A.9 *Hellisheiði Unit 2 Condensate temperature at condenser outlet*

The data for the condensate temperature shown in Figure A.9 is offset in the period before February the 26th.

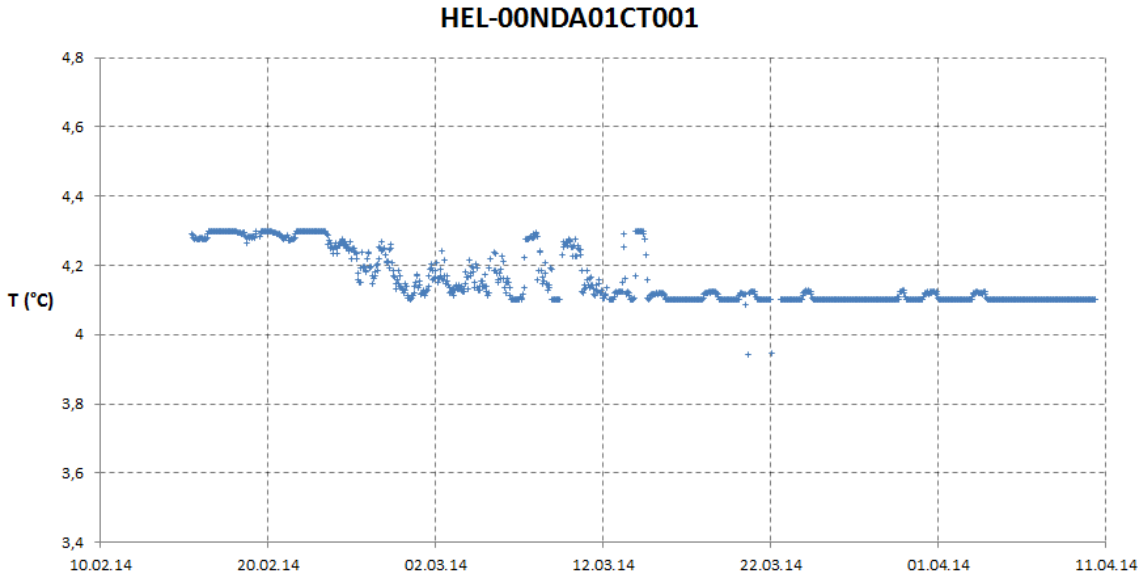

Figure A.10 *Hellisheiði Unit 2 Condenser first step: groundwater inlet temperature*

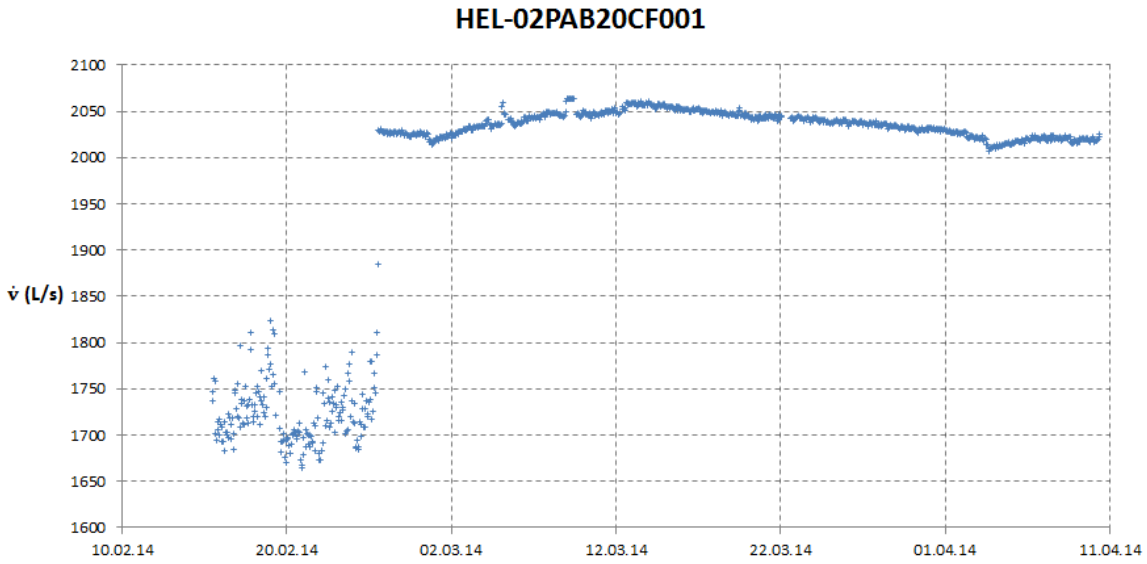

Figure A.11 *Hellisheiði Unit 2 Condenser second and third step: Cooling water flow rate*

The data for the cooling water flow rate is relatively stable after 26th of February.

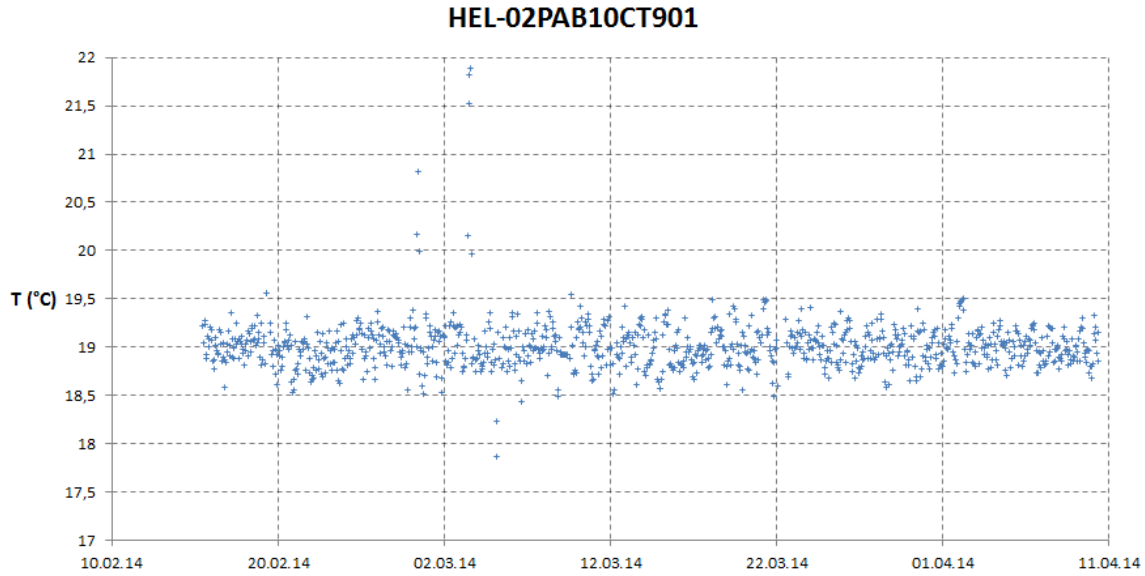

Figure A.12 *Hellisheiði Unit 2 Condenser second and third step: Cooling water inlet temperature*

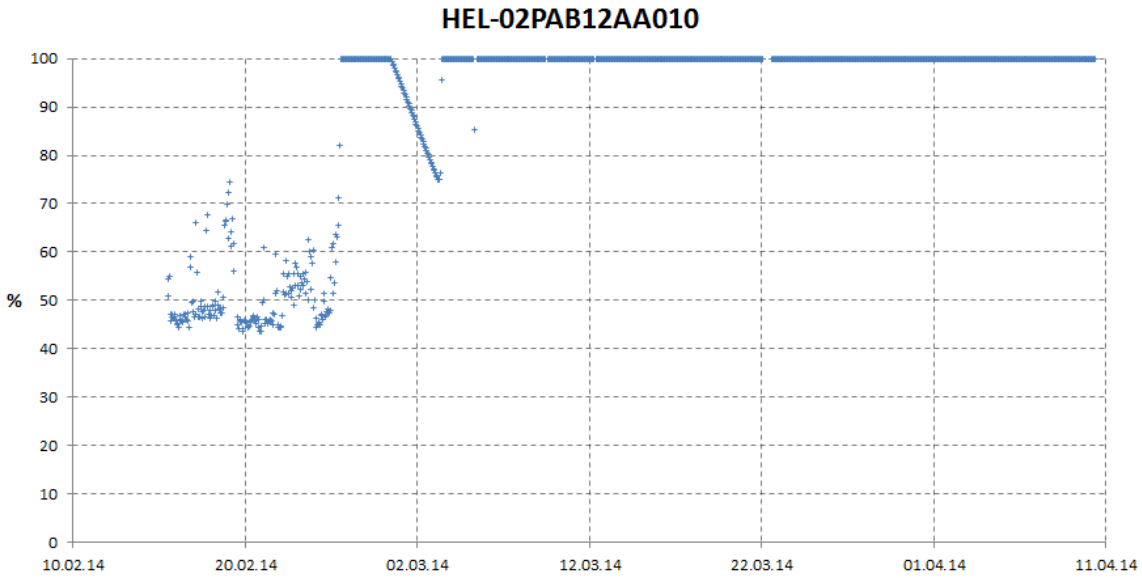

Figure A.13 *Hellisheiði Unit 2 Condenser second step: Control valve opening ratio*

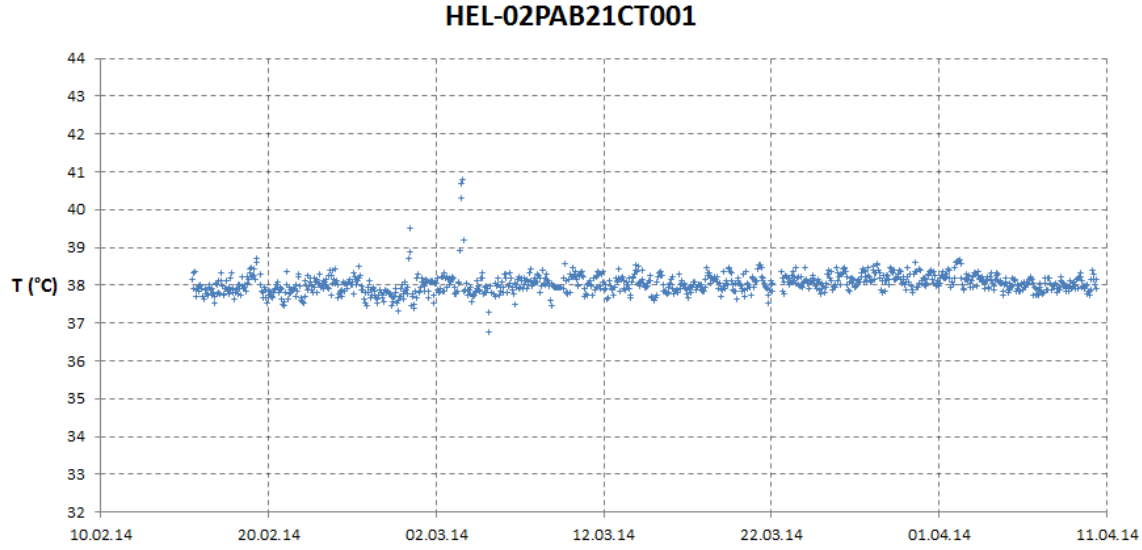

Figure A.14 *Hellisheiði Unit 2 Condenser second step: Cooling water outlet temperature*

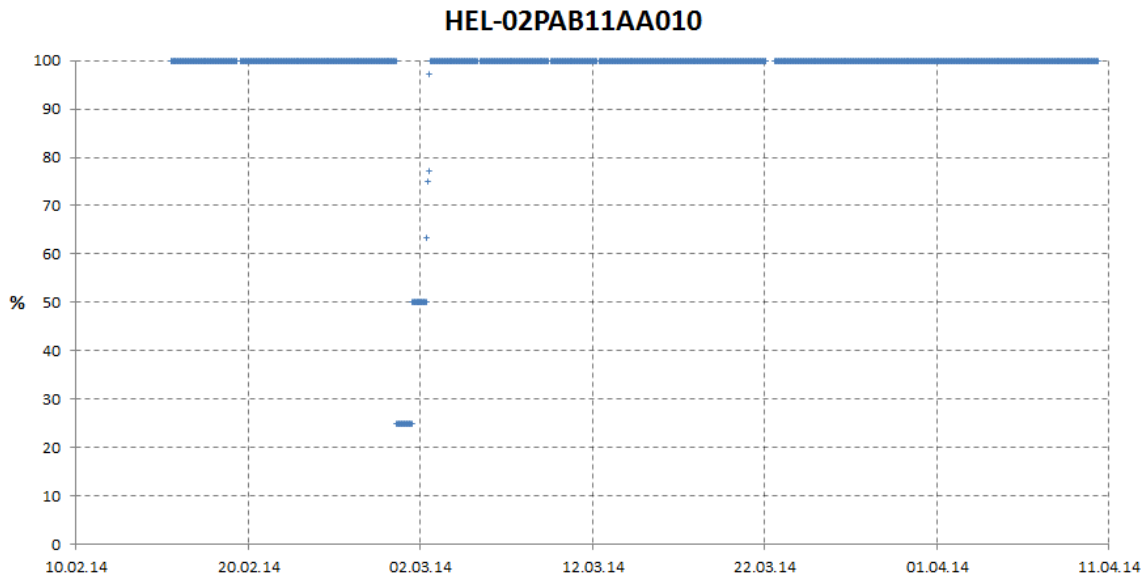

Figure A.15 *Hellisheiði Unit 2 Condenser third step: Control valve opening ratio*

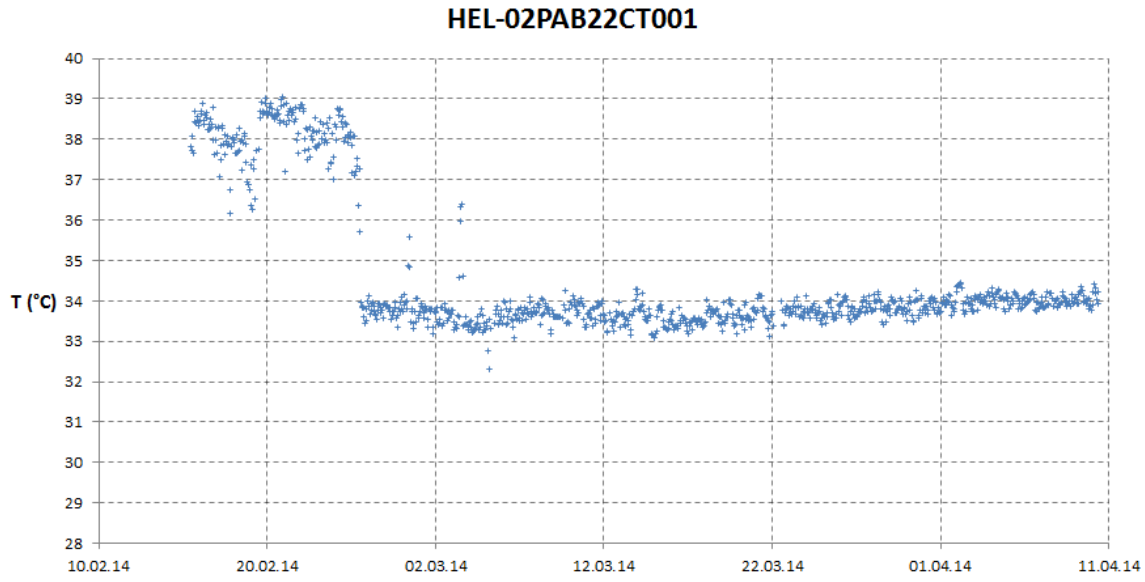

Figure A.16 *Hellisheiði Unit 2 Condenser third step: cooling water outlet temperature*

The data shown in Figure A.16 is stable after the 26th of February.

Appendix B

The following section contains the models constructed to perform the simulation

Model 1: high pressure single flash geothermal power plant cycle

"A simple model of a high pressure single flash geothermal power plant working cycle"

"Point 2: Steam separator outlet"

{Pressure in point 2} P_2 = 8,49 [bar]
{Temperature in point 2} T_2 = T_SAT(Steam;P=P_2)

{Enthalpy in point 2} h_2 = Enthalpy(steam;P=P_2;x=1)
{Entropy in point 2} s_2 = Entropy(Steam;P=P_2;x=1)
{Mass flow in point 2} m_dot_2 = 83,84 [kg/s]

“Point 22: Turbine inlet”

{Pressure at turbine inlet} P_22 = 8,36 [bar]
{Temperature} T_22 = 171,85 [C]
{Saturated temperature at P_22} T_22_sat = T_SAT(Steam;P=P_22)
{Quality in point 22} x_22 = Quality(steam;P=P_22;T=T_22)

"Point 3: Turbine outlet"

{Pressure in point 3} P_3 = 0,1152 [bar]
{Temperature in point 3:} T_3 = temperature(Steam;h=h_3;P=P_3)
{Base efficiency of the turbine} eta_0 = 0,9352
{Mass flow; NCG removal not included} m_dot_3 = m_dot_2
{Enthalpy in point 3:} h_3s = Enthalpy(Steam;P=P_3;s=s_2)
{Liquid enthalpy in point 3:} h_3l = Enthalpy(Steam;P=P_3;x=0)
{Steam enthalpy in point 3:} h_3g = Enthalpy(Steam;P=P_3;x=1)
{Steam quality in turbine outlet} x_3 = (h_2-h_3l-(eta_0-0,5)*(h_2-h_3s))/(h_3g-h_3l+(h_2-h_3s)/2)
{Total Enthalpy in point 3} h_3 = (1-x_3)*h_3l + x_3*h_3g

"Point 4"

{Enthalpy in point 4:} h_4 = Enthalpy(steam;P=P_3;x=0)
{Entropy in point 4:} s_4 = Entropy(Steam;P=P_3;x=0)
{Temperature at condenser outlet} T_4 = Temperature(water;P=P_3;x=0)
{Condenser energy transfer} Q_c = m_dot_2*(h_3-h_4)

“Turbine”

{Calculated isentropic efficiency} eta_s_calculated = (h_2-h_3)/(h_2-h_3s)
{Isentropic efficiency from manufacturer} eta_s = 0,83
{Total efficiency} eta_ = 0,786
{Comb mech and gen efficiency} eta_m_g = eta_/eta_s
{Isentropic power output} W_s = m_dot_2*(h_2-h_3s)
{Power output from data} W_data = 44290 [kW]

{Total efficiency calculated} eta_calculated = W_e/W_s
{eta_m,g,calculated} eta_m_g_calculated= eta_calculated/eta_s_calculated
{eta_m,g error} eta_m_g_error = eta_m_g_calculated/eta_m_g
{Total power output} W_e = eta_m_g*eta_s_calculated*W_s

Model 2: Includes non-condensable gases

"A simple model of a high pressure single flash geothermal power plant working cycle, including NCG"

"Point 2: Steam separator outlet"

{Pressure in point 2} P_2 = 8,49 [bar]
{Temperature in point 2} T_2 = T_SAT(Steam;P=P_2)
{Enthalpy in point 2} h_2 = Enthalpy(steam;P=P_2;x=1)
{Entropy in point 2} s_2 = Entropy(Steam;P=P_2;x=1)

“Point 22: Turbine inlet”

{Pressure at turbine inlet} P_22 = 8,36 [bar]
{Temperature} T_22 = 171,85 [C]
{Saturated temperature at P_22} T_22_sat = T_SAT(Steam;P=P_22)
{Quality in point 22} x_22 = Quality(steam;P=P_22;T=T_22)
{Mass flow in point 2} m_dot_2 = 83,84 [kg/s]

"Point 3: Turbine outlet"
{Pressure in point 3} P_3 = 0,1152 [bar]
{Temperature in point 3:} T_3 = temperature(Steam;h=h_3;P=P_3)
{Base efficiency of the turbine} eta_0 = 0,93455
{Steam mass flow } m_dot_3 = m_dot_2*(1-NCG)
{enthalpy in point 3:} h_3s = Enthalpy(Steam;P=P_3;s=s_2)
{Liquid enthalpy in point 3:} h_3l = Enthalpy(Steam;P=P_3;x=0)
{Steam enthalpy in point 3:} h_3g = Enthalpy(Steam;P=P_3;x=1)
{Steam quality in turbine outlet} x_3 = (h_2-h_3l-(eta_0-0,5)*(h_2-h_3s))/(h_3g-h_3l+(h_2-h_3s)/2)
{Total Enthalpy in point 3} h_3 = (1-x_3)*h_3l + x_3*h_3g

"NCG in turbine; NCG assumed to be CO2"
{NCG content} NCG = 0,00361
{Massflow of NCG} m_dot_NCG = m_dot_2*NCG
{Enthalpy of NCG at turbine inlet} h_2_NCG = Enthalpy(CarbonDioxide;T=T_2;P=P_2)
{Enthalpy of NCG at turbine outlet} h_3_NCG = Enthalpy(CarbonDioxide;T=T_3;P=P_3)
{Power from NCG} W_NCG = eta_0*(h_2_NCG-h_3_NCG)*m_dot_NCG

"Point 4"

{Enthalpy in point 4:} h_4 = Enthalpy(steam;P=P_3;x=0)
{Entropy in point 4:} s_4 = Entropy(Steam;P=P_3;x=0)
{Temperature at condenser outlet} T_4 = Temperature(water;P=P_3;x=0)
{Condenser energy transfer} Q_dot_c = m_dot_2*(h_3-h_4)

“Turbine”

{Calculated isentropic efficiency} eta_s_calculated = (h_2-h_3)/(h_2-h_3s)
{Isentropic efficiency from manufacturer} eta_s = 0,83
{Total efficiency} eta_ = 0,786
{comb mech and gen efficiency} eta_m_g = eta_/eta_s
{Isentropic power output} W_s = m_dot_2*(h_2-h_3s)

{Power output from data} W_data = 44290 [kW]
{Total efficiency calculated} eta_calculated = W_e/W_s
{eta_m,g,calculated} eta_m_g_calculated= eta_calculated/eta_s_calculated
{eta_m,g error} eta_m_g_error = eta_m_g_calculated/eta_m_g
{Total power output} W_e = eta_m_g*(eta_s_calculated*W_s + W_NCG)

Model 3: Cold end model of the condenser

"Point 3: Condenser step 1, steam inlet"

{Pressure} P_3 = 0,1152 [bar]
{Temperature} T_3 = T_SAT(Steam;P=P_3)
{Mass flow} m_dot = 83,84 [kg/s]
{NCG content} NCG = 0,00361

{0,361% of the massflow is from non condensable gases that are removed at the top of the condenser}
{Assuming that no steam leaves the condenser with the NCG's}

{Steam mass flow} m_dot_3 = m_dot*(1-NCG)

"Point 8: Condenser step 1, ground water inlet"

{Volume flow} v_dot_8 = 221 [L/s]
{Temperature} T_8 = 4,15 [C]
{Pressure} P_8 = 1,9 [bar]
{Average temperature} T_8_avg = (T_8+T_9)/2
{Density} rho_8 = Density(Water;P=P_8;T=T_8)
{Massflow} m_dot_8 = v_dot_8*rho_8*0,001 [kg/s]
{Enthalpy} h_8 = Enthalpy(water;T=T_8;x=0)

"Point 9: Condenser step 1, ground water outlet"

{Mass flow} m_dot_9 = m_dot_8
{Temperature} T_9 = 43,69 [C]
{Enthalpy} h_9 = Enthalpy(water;T=T_9;x=0)

"Point 10: Condenser step 2, steam inlet"

{Mass flow} m_dot_10 = m_dot_3
{Temperature} T_10 = T_3

"Condenser step 1: Overall heat transfer coefficient and energy transfer"

{Area of exchange} A_1 = 2775 [m^2]
{Exchanger Effectiveness} epsilon_1 = (T_9-T_8)/(T_3-T_8)
{Specific heat of cooling water} c_8 = Specheat(Water;T=T_8_avg;P=P_8)
{NTU} epsilon_1 = 1-(exp(-N_1))
{Heat transfer coefficient} 1000*N_1 = U_1*A_1/(m_dot_8*c_8)
{Heat transfer} Q_dot_c1 = m_dot_8*c_8*(T_9-T_8)
{Heat transfer} Q_dot_c11 = m_dot_8*(h_9-h_8)

"Point 11: Condenser step 2, cooling water outlet"

{Mass flow} m_dot_11 = m_dot_12
{Temperature} T_11 = 38,06 [C]
{Enthalpy} h_11 = Enthalpy(Water;T=T_11;x=0)

"Point 12: Condenser step 2, cooling water inlet"

{Valve opening} o_12 = 99,1 [%]
{Valve opening ratio} r_12 = o_12/(o_12+o_15)
{mass flow} m_dot_12 = m_dot_17*r_12
{Pressure} P_12 = 1,9 [bar]
{Temperature} T_12 = T_17
{Average temperature} T_12_avg = (T_12+T_11)/2
{Enthalpy} h_12 = Enthalpy(Water;T=T_12;x=0)

"Condenser step 2: Overall heat transfer coefficient and energy transfer"

{Area of exchange} A_2 = 1548 [m^2]
{Exchanger Effectiveness} epsilon_2 = (T_11-T_12)/(T_10-T_12)
{Specific heat of cooling water} c_12 = Specheat(Water;T=T_12_avg;P=P_12)
{NTU} epsilon_2 = 1-(exp(-N_2))
{Heat transfer coefficient} 1000*N_2 = U_2*A_2/(m_dot_12*c_12)
{Heat transfer} Q_dot_c2 = m_dot_12*c_12*(T_11-T_12)
{Heat transfer} Q_dot_c22 = m_dot_12*(h_11-h_12)

"Point 13: Condenser step 3, steam inlet"

{Mass flow} m_dot_13 = m_dot_3
{Temperature} T_13 = T_10

"Point 14: Condenser step 3, cooling water outlet"

{Massflow} m_dot_14 = m_dot_15
{Temperature} T_14 = 33,77 [C]
{Enthalpy} h_14 = Enthalpy(Water;T=T_14;x=0)

"Point 15: Condenser step 3, cooling water inlet"

{Valve opening} o_15 = 97,31 [%]
{Valve opening ratio} r_15 = o_15/(o_15+o_12)
{mass flow} m_dot_15 = m_dot_17*r_15
{Temperature} T_15 = T_17
{Average temperature} T_15_avg = (T_15+T_14)/2
{Pressure} P_15 = 1,9 [bar]
{Enthalpy} h_15 = Enthalpy(Water;T=T_15;x=0)

"Point 16: Condenser step 2 and 3, combined outlet"

{Mass flow} m_dot_16 = m_dot_11 + m_dot_14

"Point 17: Condenser step 2 and 3, combined inlet "

{Volume flow} v_dot_17 = 2036 [L/s]
{Pressure} P_17 = 1,9 [bar]
{Temperature} T_17 = 19,02 [C]
{Density} rho_17 = Density(Water;P=P_17;T=T_17)
{Massflow} m_dot_17 = v_dot_17*rho_17*0,001 [kg/s]

"Condenser step 3: Overall heat transfer coefficient and energy transfer"

{Area of exchange} A_3 = 2396 [m^2]
{Exchanger Effectiveness} epsilon_3 = (T_14-T_15)/(T_13-T_15)
{Specific heat of cooling water} c_15 = Specheat(Water;T=T_15_avg;P=P_15)
{NTU} epsilon_3 = 1-(exp(-N_3))
{Heat transfer coefficient} 1000*N_3 = U_3*A_3/(m_dot_15*c_15)
{Heat transfer} Q_dot_c3 = m_dot_15*c_15*(T_14-T_15)

{Heat transfer} Q_dot_c33 = m_dot_15*(h_14-h_15)

"Condenser all steps: Total energy transfer"

{Total heat transfer} Q_dot_c = Q_dot_c1+Q_dot_c2+Q_dot_c3
Q_dot_total2 = Q_dot_c11+Q_dot_c22+Q_dot_c33

"Point 4: Condenser step 3, condensate outlet "

{Massflow} m_dot_4 = m_dot_13
{Temperature} T_4 = Temperature(steam;P=P_3;h=h_4)
{Enthalpy} h_4 = Enthalpy(Steam;P=P_3;x=0)
{Steam quality} x_4 = Quality(steam;P=P_3;h=h_4)

"Point 3: Condenser steam inlet"

"Q_dot_c = m_dot_3*(h_3-h_4)"
{Enthalpy} h_3 = (Q_dot_c/m_dot_3) + h_4
{Quality} x_3 = Quality(steam;P=P_3;h=h_3)

"Estimating the Overall heat transfer coefficient of a combined in and outlet"

"Point 8"
{Specific heat in point 8} c_p8 = Specheat(Water;T=T_8;P=P_8)
{Energy in point 8} Q_dot_8 = m_dot_8*c_p8*(T_8+273,15)

"Point 9"
{Pressure} P_9 = 1,9 [bar]
{Specific heat in point 9} c_p9 = Specheat(Water;T=T_9;P=P_9)
{Energy in point 9} Q_dot_9 = m_dot_9*c_p9*(T_9+273,15)

"Point 11"
{Pressure in point 11} P_11 = 1,9 [bar]
{Specific heat in point 11} c_p11 = Specheat(Water;T=T_11;P=P_11)
{Energy in point 11} Q_dot_11 = m_dot_11*c_p11*(T_11+273,15)

"Point 12"
{Specific heat in point 12} c_p12 = Specheat(Water;T=T_12;P=P_12)
{Energy in point 12} Q_dot_12 = m_dot_12*c_p12*(T_12+273,15)

"Point 14"
{Pressure in point 14} P_14 = 1,9 [bar]
{Specific heat in point 14} c_p14 = Specheat(Water;T=T_14;P=P_14)
{Energy in point 14} Q_dot_14 = m_dot_14*c_p14*(T_14+273,15)

"Point 15"
{Specific heat in point 15} c_p15 = Specheat(Water;T=T_15;P=P_15)
{Energy in point 15} Q_dot_15 = m_dot_15*c_p15*(T_15+273,15)

"Point 16: Combining outlets 11 and 14"
{Pressure in point 16} P_16 = 1,9 [bar]
{Specific heat in point 16} c_p16 = (c_p11+c_p14)/2
{Energy in point 16} Q_dot_16 = Q_dot_11+Q_dot_14
{Temperature in point 16} T_16 = Q_dot_16/(m_dot_16*c_p16) - 273,15

"Point 17"
{Specific heat in point 11} c_p17 = Specheat(Water;T=T_17;P=P_17)
{Energy in point 11} Q_dot_17 = m_dot_17*c_p17*(T_17+273,15)

"Combined inlet"

{Mass flow}	m_dot_in = m_dot_8+m_dot_17
{Energy}	Q_dot_in = Q_dot_8 + Q_dot_17
{Specific heat}	c_p_in = (m_dot_8*c_p8 + m_dot_17*c_p17)/(m_dot_8+m_dot_17)
{Temperature}	T_in = Q_dot_in/(m_dot_in*c_p_in) - 273,15

"Combined outlet"

{Mass flow}	m_dot_out = m_dot_9 + m_dot_16
{Energy}	Q_dot_out = Q_dot_9 + Q_dot_16
{Specific heat}	c_p_out = (m_dot_9*c_p9 + m_dot_16*c_p16)/(m_dot_9 + m_dot_17)
{Temperature}	T_out = Q_dot_out/(m_dot_out *c_p_out) - 273,15

"Condenser: Combined steps 1-3"

{Area of exchange}	A = 2396 + 1548 + 2775 [m^2]
{Exchanger Effectiveness}	epsilon_= (T_out-T_in)/(T_3-T_in)
{Avg cooling water temp}	T_avg = (T_in + T_out)/2
{Specific heat of cooling water}	c = Specheat(Water;T=T_avg;P=P_17)
{NTU}	epsilon_ = 1-(exp(-N))
{Heat transfer coefficient}	1000*N = U*A/(m_dot_in*c)
{Heat transfer}	Q_dot_comb = m_dot_in*c*(T_out-T_in)